Transaction B: Mechanical Engineering
Vol. 16, No. 5, pp. 387–412


# Dynamic Model of a Mobile Robot with Long Spatially Flexible Links

**H. Zohoor**[1,*] **and S.M. Khorsandijou**[2]

**Abstract.** *Using some agent variables, the general structure of the dynamic model of a spatial mobile robot with $N$ long spatially flexible links and $N$ revolute joints has been exposed. It is composed of a set of $5N+6$ nonlinear coupled partial differential motion equations under the influence of the boundary conditions. Non-conservative forces/moments have been neglected. While being considered, the general structure of the dynamic model will not change, but a few exciting/damping terms will arise within the agent variables. The base of the robot is an unconstrained rigid body in space and the links as 3D Euler-Bernoulli beams undergo tension-compression, torsion and two spatial bendings while elastic orientation is considerable and the nonlinear part of the geometric Green-Lagrange strain is ignored. When the elastic orientation is neglected, the dynamic model of each link remains more accurate than that of a nonlinear 3D Euler-Bernoulli beam within which the elastic orientation is actually negligible. The obtained dynamic model is capable of creating the nonlinear 3D long Euler-Bernoulli beam and the fully-enhanced/enhanced/generalized nonlinear 3D Euler-Bernoulli beam theories, considering a flying or a fixed support.*

**Keywords:** *Spatially flexible link; Highly flexible link; Mobile robot; Flying manipulator.*

## INTRODUCTION

In mobile robots, the link's elastic deformations can be revealed by accelerations of the mobile base and manipulator, the length and mechanical flexibility of the links and the mass ratio of payload to manipulator. When the link's elastic deformations are predicted to be considerable, the links should not be considered as rigid in the dynamic modeling. The dynamic modeling and configuration determining of a flexible-link mobile robot are sophisticated kinetic problems. As the length and mechanical flexibility of the links increase, the elastic orientation becomes considerable. As a result, the links cannot be modeled as nonlinear 3D Euler-Bernoulli beams like [1-3] within which the elastic orientation is negligible.

In the present article and in [4], spatially flexible links undergoing considerable elastic orientation are named long links. Using some agent variables, the general structure of a dynamic model of a spatial mobile robot with $N$ revolute joints and $N$ long links has been obtained. It includes the partial differential motion equations, section loads of the links and the boundary conditions of the system. Each link undergoes four independent elastic deformations, namely torsion, tension/compression and two spatial bendings. In the present article, the agent variables whose lengths are independent of $N$, are determined for any $N$, and the agent variables whose lengths are dependent upon $N$ are determined only for $N=2$. It should be noted that only the appearance of agent variables whose lengths are dependent upon $N$ for $N=2$ is similar to that of [4] within which the elastic orientation is negligible. Obviously, these agent variables can be reduced to that of [4] if the rotational elastic coordinates are replaced by zero.

The novelty of the present article and [4] lies not only in the large spatial flexibility of the long links, but also in the dynamic model itself, regardless of the links' quality of flexibility. This dynamic model is in fact a unification for the dynamic models of flying and/or fixed-base robots and/or multiple pendulums with rigid

1. *Center of Excellence in Design, Robotics and Automation, Sharif University of Technology, Tehran; and The Academy of Sciences, Tehran, Iran.*
2. *School of Mechanical Engineering, Sharif University of Technology, Tehran, Iran.*
*. *Corresponding author. E-mail: zohoor@sharif.edu*

*Received 20 February 2008; received in revised form 29 August 2008; accepted 14 October 2008*

and/or flexible links serially connected by revolute joints, one flying rigid body, and long and/or short fully-enhanced and/or short enhanced and/or short generalized nonlinear 3D and/or 2D Euler-Bernoulli beams with a flying and/or a fixed support. The mentioned unification has been achieved using the agent variables of the present article. Several examples have been cited in section of "Verification of the Dynamic Model".

A system is flexible anyway, depending on the time scale of the task to be solved and on the length scale of the needed dynamic accuracy [5]. Typically, the deflections are dynamic and arise as vibrations. The philosophies of arm structure design have been explained by Book [5]. Putz [6] has clarified the major differences between space and terrestrial mobile robots. Any mechanically flexible manipulators/structures are inherently distributed parameter systems whose dynamics are described by partial, rather than ordinary, differential equations [7].

Kakizaki et al. [8] have presented a dynamic modeling method for spatial elastic manipulators that can account for bearing clearances, actuator dynamics and control system characteristics. The dynamics of an orbiting platform supporting a multi-link flexible manipulator system is derived by Modi et al. [9], while the links are modeled as Timoshenko beams. Karray et al. [10] have obtained the motion equations of an orbiting flexible manipulator while the two flexible manipulator links, treated as Euler-Bernoulli beams, are free to deform transversely in the orbital plane. In the framework of a linear elasticity theory, Hiller [11] has modeled the flexible parts of arm elements as Euler-Bernoulli beams. Two bending deflections and a so-called twisting angle are considered as three elastic degrees of freedom while inner constraints have been assumed for axial deformation and the so-called bending rotation angles. Korayem and Ghariblu [12] have considered a planar small deflection for the link of a wheeled mobile flexible manipulator.

Using some agent variables, Khorsandijou and Zohoor [4] have exposed the general structure of the dynamic model of a spatial mobile robot with $N$ highly flexible links and $N$ revolute joints, that is a set of $5N + 6$ nonlinear coupled partial differential equations, along with boundary conditions. The agent variables whose lengths are independent of $N$ have been determined for any $N$ when the links undergo considerable and also negligible, elastic orientation. When $N = 2$ and the elastic orientation is negligible, all fifty agent variables of the general structure of the dynamic model have been determined. When the flexibility of the links is ignored, the dynamic model is reduced to a set of $N + 6$ nonlinear coupled ordinary differential equations. Non-conservative forces and moments are neglected, but if they are considered, the general structure of the dynamic model will not change. In [4], the base of the robot is a six-DoF rigid body in space and each link, as an Euler-Bernoulli beam has whole elastic spatial degrees of freedom, i.e. tension compression, torsion and two spatial bendings. The links are made from a linearly elastic isotropic material and are dynamically modeled much more accurately than those of a nonlinear 3D Euler-Bernoulli beam. That is, the elastic orientation of the cross-sectional frame of each link is considerable. Moreover, when the elastic orientation of the cross-section is neglected, the dynamic model of each link remains more accurate than that of a nonlinear 3D Euler-Bernoulli beam. These findings have enhanced the conventional nonlinear 3D Euler-Bernoulli beam theory within which the elastic orientation of the cross-sectional frame is actually negligible. In [4], the variation of elastic potential energy of long links has been used to derive the links' fully-enhanced/enhanced variation of elastic potential energy, within which the elastic orientation is negligible. In [4], the primary and secondary new elastic terms have been revealed to improve the nonlinear 3D Euler-Bernoulli beam theory in [1]. Zohoor and Khorsandijou [13] have exposed the dynamic model of a flying manipulator with two highly flexible links within which the flexibility has been modeled as that of [2]. The dynamic model in [13] includes sixteen coupled nonlinear partial differential motion equations along with the boundary conditions.

A method is presented by Sunada and Dubowsky [14] for analyzing the complete behavior of industrial robotic manipulators with complex-shape flexible links including the effects of the manipulator's control systems and actuators. The kinematics and dynamics of the manipulator are expressed in terms of 4 multiplied by 4 matrices. The distributed flexibility and mass properties of the links are obtained by using readily available finite-element models and programs [14]. Nonlinear equations of motion are developed by Book [15] for flexible manipulator arms consisting of rotary joints that connect pairs of flexible links. The kinematics of both the rotary-joint motion and the link deformation are described by 4 multiplied by 4 transformation matrices. The link deflection is assumed small, so that the link transformation can be composed of the summations of assumed link shapes. Cetinkunt et al. [16] have presented a method to derive symbolically the full nonlinear dynamic equations of motion of multiple-link flexible manipulators. Lagrange's-assumed modes method is used for the dynamic modelling. The design of lightweight links for robotic manipulators results in flexible links [17]. The accurate control of lightweight manipulators during the large changes in configuration common to robotic tasks requires dynamic models that describe both rigid-body motions as well as flexural vibrations [17]. In this relation, Hastings and Book [17] have described a linear state-space model for a single-link flexible manipulator. Dubowsky et al. [18] have presented an effective method for modeling the full three-dimensional dynamics of high performance spatial machine systems including the vibrations of their links, supporting structure and enclosures and impacts in their connection clearances. The method combines four-by-four matrix modeling techniques with finite-element techniques. The lightweight flexible manipulator dynamics are derived by Siciliano and Book [19] on the basis of a Lagrangian-assumed modes method. The explicit, non-recursive symbolic form of the dynamic model of robotic manipulators with compliant links and joints is developed by Cetinkunt and Book [20] based on a Lagrangian-assumed mode of formulation. This form of dynamic model is suitable for controller synthesis as well as accurate simulations of robotic applications. The final form of the equations is organized in a form similar to rigid manipulator equations. Dubowsky [21] has described an approach to modeling the flexibility effects in spatial mechanisms and manipulator systems. The method is based on finite element representations of the individual links in the system. However, it should be noted that conventional finite element methods and software packages will not handle the highly nonlinear dynamic behavior of these systems [21]. Book [22] has represented the dynamics of the link by the Euler-Bernoulli beam equation. Matsuno and Yamamoto [23] have approximated the elastic deformations by means of B-spline functions and have derived dynamic equations of joint angles, the vibration of the flexible link and the constraint force. Matsuno et al. [24] have derived dynamic equations of joint angles, vibrations of flexible links and the contact force, by means of Hamilton's principle. Rocco and Book [25] have obtained a finite dimensional model of a robot by truncating the modal expansion of the deflection to a finite number of assumed modes, under the assumption of small deformation. Bernzen et al. [26] have presented an effective way for numerical modelling of multilink flexible robots. Shi et al. [27] have used an Euler-Bernoulli beam to model the flexible link where the rotary-inertia and shear-deformation effects are neglected and the elastic deformation is assumed to be small [27]. Chen [28] has presented a linearized dynamic model for a multi-link planar flexible manipulator which can include an arbitrary number of flexible links. The elastic deformation of each link is modeled by using the assumed-mode method. Flexible links are treated as Euler-Bernoulli beams and rotary inertia and shear deformation are thus neglected. Siciliano and Villani [29] have modeled planar $n$-link flexible manipulators using the Euler-Bernoulli beam equation and the assumed modes technique.

Since the flexibility of robotic links might be appropriately modeled by beam or rod theories, the literature survey of the present article has been enriched by papers concentrating on beams and rods.

Using the assumed mode method and Lagrangian approach, Tan et al. [30] have derived the equations of motion of a rotating cantilever Euler-Bernoulli beam subjected to base excitation. Shi et al. [31] have found that the traditional deformation field, used for Euler-Bernoulli beams, fails to produce an elastic rotation matrix that is complete to second-order in the deformation variables. They have proposed a complete second-order deformation field along with the equations needed to incorporate the beam model into a graph-theoretic formulation for flexible multibody dynamics. They have presented two examples to demonstrate the effects of the proposed second-order deformation field on the response of a flexible multibody system. Nayfeh and Pai [1] have presented linear shear-deformable beam theories; the linear Euler-Bernoulli beam theory, the nonlinear 2D Euler-Bernoulli beam theory, the nonlinear 3-D curved beam theory, accounting for warpings and the nonlinear 3-D Euler-Bernoulli beam theory. Yang et al. [32] have investigated the flexible motion of a uniform Euler-Bernoulli beam attached to a rotating rigid hub. Fully coupled nonlinear integro-differential equations describing the axial, transverse and rotational motions of the beam are derived by using the extended Hamilton's principle.

Zohoor and Khorsandijou [2] have derived the boundary conditions and the ten coupled nonlinear partial differential motion equations of an enhanced nonlinear 3D Euler-Bernoulli beam with flying support. This beam undergoes negligible elastic orientation. In [2] some new elastic terms that would not be sensed in the nonlinear 3D Euler-Bernoulli beam theory are exposed. In [3], the existence of some other new elastic terms [33] have been pointed to which have been sensed neither in the nonlinear 3D Euler-Bernoulli beam theory [1] nor in [2], thereby improving both the nonlinear 3D Euler-Bernoulli beam theory as shown in [1], and the enhanced nonlinear 3D Euler-Bernoulli beam theory as shown in [2].

Novozhilov [34] has studied the deformation of thin prismatic rods of an arbitrary cross-section. He has considered 1st and 2nd order approximations for the displacement components of an arbitrary point of a cross-section using Taylor-series expansions in terms of the two components of the position vector of the arbitrary point apparent in the cross-sectional frame. Strain components are derived from these approximated displacements. Green and Laws [35] have shown that a rod theory, defined as a curve to every point of which a rotation vector is attached, is a special constrained case of a rod theory in which two deformable directors are attached to each point of a curve. Some aspects of both the linear and nonlinear theories of elastic rods are discussed by Green et al. [36] via the three-dimensional theory of classical continuum mechanics. Constitutive equations for the linear isothermal theory of elastic rods of an isotropic material and of variable cross-sections are derived by an approximation procedure from the three-dimensional equations in [36] and by a direct approach based on the theory of a Cosserat curve with two directors in [37]. Green et al. [37] have developed the linear isothermal theory of straight isotropic rods of variable cross-sections possessing two axes of symmetry. Antman [38] has formulated a general theory of nonlinearly elastic rods of sufficient geometric structure to allow not only for flexure and torsion, as in the Kirchhoff theory, but also for the axial extension and shear of the cross-section with respect to the axis. Whitman and DeSilva [39] have developed a three dimensional nonlinear equilibrium theory of elastic rods applicable to large displacements and small strains, and accounting for extensibility and shear deformation. Utilizing a nonlinear theory of rods which is formulated on the basis of a Cosserat curve with two directors, a number of constrained theories of various degrees of generality are developed by Naghdi and Rubin [40]. In addition to the nonlinear version of the Euler-Bernoulli beam theory, six other less restrictive nonlinear constrained theories are also discussed [40]. Steigmann and Faulkner [41] have presented the simplest theory of spatial rods. O'Reilly and Turcotte [42] have developed and analyzed a model for the deformation of a rotating prismatic rod-like body.

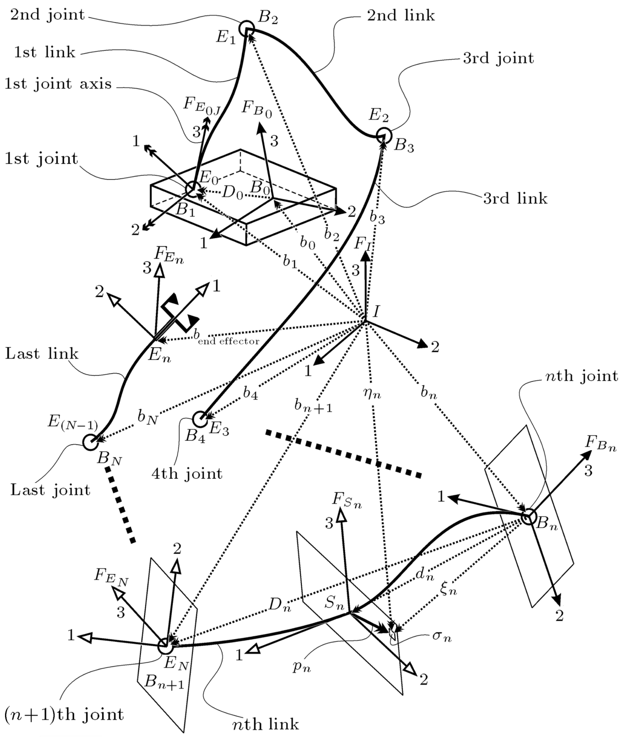


**Figure 1.** Mobile robot with long links [13].

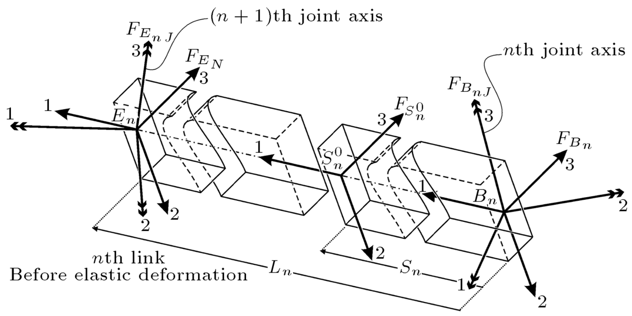


**Figure 2.** An undeformed long link [13].

## ASSUMPTIONS

As shown in Figure 1, the spatial mobile robot has $N$ revolute joints and $N$ long links. Since the present article concentrates on the elastic and inertia terms, non-conservative forces/moments and probable contact constraints have been neglected. The mobile base of the robot is assumed to be a rigid body with six flying DoF (Degrees of Freedom). As shown in Figures 2-4, the links are straight before elastic deformation, and the non-functional variable, $s_n$, is a Lagrangian rather than Eulerian coordinate. The links are made from an isotropic linearly elastic material with uniform density and cross-section. The frames, shown by Figures 1-5, are assumed to be right-handed orthogonal and their axes are marked by numbers, namely 1, 2 and 3, to indicate the 1st, 2nd and 3rd axes, respectively.

The link's cross-sectional frame, $F_{s_n}$, is a curvilinear orthogonal right-handed coordinate frame having a 1st axis tangent to the curve created by cross-sectional area centers. It is assumed to be a principal cross-sectional frame, having the same moments of area about the 2nd and 3rd axes. In other words, the links might be imagined with circular and/or square cross-sections. The following equation shows the rotary cross-sectional area tensor of the links:

$$[J_{S_n}] = J \begin{bmatrix} 2 & 0 & 0 \\ 0 & 1 & 0 \\ 0 & 0 & 1 \end{bmatrix}. \tag{1}$$

Each link, as an Euler-Bernoulli beam, experiences torsion, tension/compression and two spatial bendings. Since the Euler-Bernoulli beam is the most rigid beam compared to the other beams, it is assumed that the links' shear deformation does not exist. The links' cross-section is supposed to remain plane and perpendicular to the center line before and after elastic deformations. It implies Bernoulli's hypothesis that

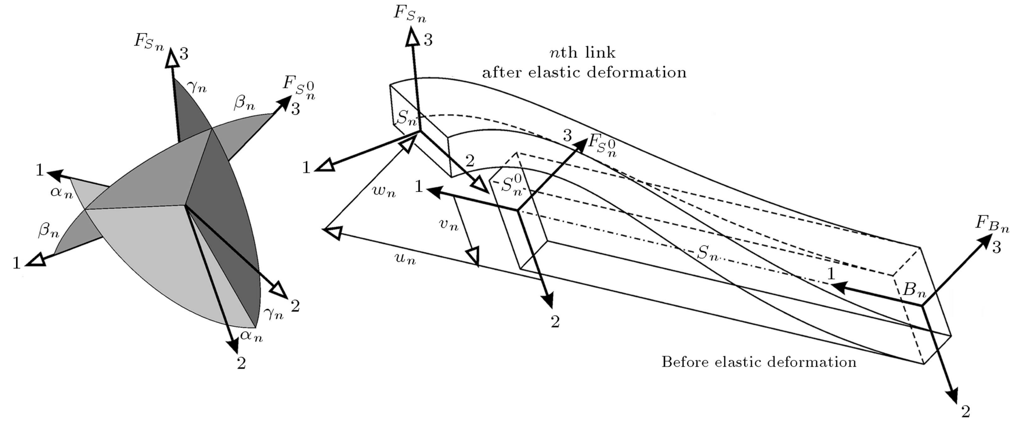


**Figure 3.** Six dependent elastic coordinates for a long link [2,13].

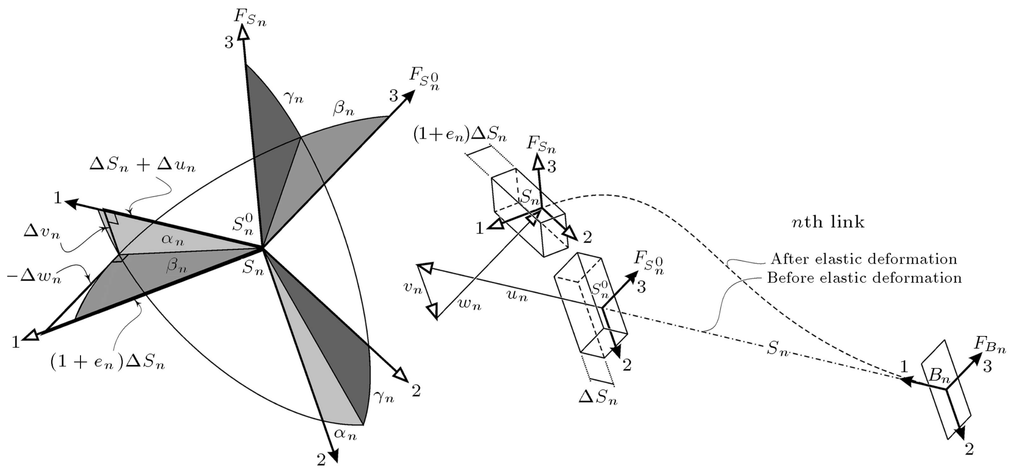


**Figure 4.** Two holonomic constraints among the elastic coordinates of a long link [3,4].

neglects the out-of-plane warping of the cross-section. The links are assumed to be long, that is, the elastic orientation of them is assumed to be considerable and thus cannot be neglected. This assumption is one of the particular novelties of this article. In the present article and in [1-4,13,33], the partial differentiations of displacement field with respect to the Lagrangian cross-sectional coordinates, i.e. $\partial\Delta_n/\partial y_n$ and $\partial\Delta_n/\partial z_n$, have been ignored, and the exact linear part of the Green-Lagrange geometric strain tensor is considered as the links'/beam's strain. However, the effect of the ignored items will be analyzed later.

The links experience torsion beyond bending and axial deformation. As a result, the out-of-plane warping of the cross-section should arise according to Saint Venant's theory of torsion. It should be noted that spatial bending induces torsion even in isotropic beams. As a result, according to Bernoulli's hypothesis and the Saint Venant theory of torsion, the assumption is accurate for slender beams with a circular cross-section, and inaccurate for other cross-sections. The in-plane warping of the beam cross-section has been neglected. In this regard, the Poisson ratio might be substituted with zero in the formulations, but since the stress in the links is treated three dimensionally, the Poisson ratio in the formulations has not been substituted with zero in this article. As a result, components of the vector, $p_n$, shown by Figures 1-5, are assumed to be constant. This implies that the in-plane and out-of-plane warping of the links' cross-section has been ignored.

## KINEMATICS

Figure 1 shows that the mobile base of the robot is connected to the 1st link by the 1st revolute joint. The mobile robot has $N$ revolute joints and $N$ long spatially flexible links, being sequentially connected to each other. The end frame of the last link is the end-effector of the robot. The dynamic modelling of the robot requires the kinematical parameters that are derived in this section.

As a matter of fact, each link, as a deformable

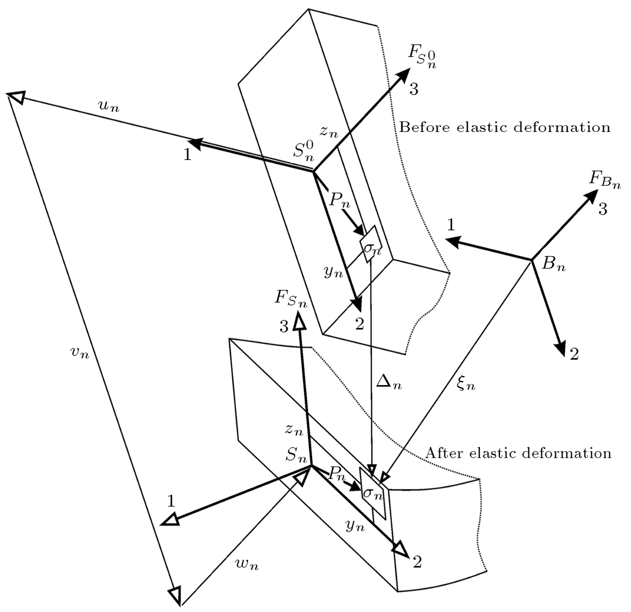


**Figure 5.** Elastic displacement field of a long link.

continuous medium, has infinite elastic DoF being mathematically described by four independent elastic DoF. The mentioned four independent elastic DoF are functions of the non-functional variable, namely $s_n$, while $0 \leq s_n \leq L_n$. The mobile base and revolute joints have, respectively, 6 and $N$ independent DoF so it can be found that the DoF of the robot is mathematically equal to $6 + 5N$.

### Mobile Base

Absolute virtual rotation, i.e. Equation 2, and the angular velocity of the mobile base of the robot are required for the scope of this article. Virtual rotation and angular velocity are, respectively, imperfect differential and non-integrable time-derivative.

$$\delta\pi^{B_0} = \begin{bmatrix} 1 & 0 & -\sin\phi_0 \\ 0 & \cos\psi_0 & \sin\psi_0\cos\phi_0 \\ 0 & -\sin\psi_0 & \cos\psi_0\cos\phi_0 \end{bmatrix} \begin{bmatrix} \delta\psi_0 \\ \delta\phi_0 \\ \delta\theta_0 \end{bmatrix}. \tag{2}$$

### Representative Point of the Links' Cross-Section

The representative point of the links' cross-section, i.e. $\sigma_n$, has been shown by Figures 1 and 5. The kinematical parameters of the representative point of the cross-section of the $n$th link are given in this section. They are used in deriving the variation of the elastic/gravitational potential energy and the variation of the kinetic energy of the links. The apparent position and apparent virtual displacement of $\sigma_n$ in $F_{B_n}$ are, respectively, given by Equations 3 and 4, which are projected onto $F_{B_n}$.

$$\xi_n = d_n + \underset{B_nS_n}{R}\, p_n, \tag{3}$$

$$\delta\xi_n = \delta d_n - \underset{B_nS_n}{R}\, \widetilde{p_n}\delta\Pi^{S_n} = \begin{bmatrix} \delta u_n & \delta v_n & \delta w_n \end{bmatrix}^T + \underset{B_nS_n}{R}\begin{bmatrix} (z_n\delta\Pi_{n_y} - y_n\delta\Pi_{n_z}) & -z_n\delta\Pi_{n_x} & y_n\delta\Pi_{n_x} \end{bmatrix}^T. \tag{4}$$

The absolute acceleration and absolute virtual displacement of $\sigma_n$ are, respectively, given by Equations 5 and 6, which are projected onto $F_{B_n}$.

$$\underset{B_n}{a}^{\sigma_n} = \underset{B_nI}{R}\,\ddot{\eta}_n = \underset{B_nI}{R}\,\underset{I}{a}^{B_n} + \ddot{\xi}_n + 2\widetilde{\omega}^{B_n}\dot{\xi}_n + \widetilde{\omega}^{B_n}\widetilde{\omega}^{B_n}\xi_n + \dot{\widetilde{\omega}}^{B_n}\xi_n, \tag{5}$$

$$\underset{B_nI}{R}\,\delta\eta_n = \underset{B_nI}{R}\,\delta b_n + \delta d_n - \underset{B_nS_n}{R}\,\widetilde{p_n}\delta\Pi^{S_n} + \delta\widetilde{\pi}^{B_n}\left(d_n + \underset{B_nS_n}{R}\, p_n\right). \tag{6}$$

### Long Spatially Flexible Links

Figure 3 simply describes the spatial elastic deformation of the $n$th link, using six elastic coordinates, namely, $u_n, v_n, w_n, \alpha_n, \beta_n$ and $\gamma_n$. The Euler angles, $\alpha_n, \beta_n$ and $\gamma_n$ have been called Bryant angles in [11]. The two holonomic constraints of Equations 7 and 8 are the link structural constraints derived from the two right triangles in the left-hand-side of Figure 4. In this article, $u_n, v_n, w_n$ and $\gamma_n$ have been considered as the elastic DoF of the $n$th link, because of the fact that each superfluous coordinate of a holonomic system can be eliminated together with a holonomic constraint.

The elastic orientation of the long links is considerable, thus $\alpha_n, \beta_n, \gamma_n$ or $v'_n, w'_n, \gamma_n$ cannot be ignored and eventually the links cannot be modeled as a nonlinear 3D Euler-Bernoulli beam [1], which in fact neglects elastic orientation.

$$\alpha_n = \lim_{\Delta s_n \to 0} \tan^{-1}\frac{\Delta v_n}{\Delta s_n + \Delta u_n} = \tan^{-1}\frac{v'_n}{h_n}, \tag{7}$$

$$\beta_n = \lim_{\Delta s_n \to 0} \tan^{-1}\frac{-\Delta w_n}{\sqrt{(\Delta s_n + \Delta u_n)^2 + \Delta v_n^2}} = -\tan^{-1}\frac{w'_n}{r_n}. \tag{8}$$

Figure 4 validates Equation 9, which is used to derive the centerline axial strain of the $n$th link, i.e. Equation 10.

$$\underset{S_nB_n}{R}\left[(\Delta s_n+\Delta u_n) \quad \Delta v_n \quad \Delta w_n\right]^T$$

$$=(e_n+1)\Delta s_n\left[1 \quad 0 \quad 0\right]^T, \tag{9}$$

$$e_n=\sqrt{(1+u_n')^2+v_n'^2+w_n'^2}-1. \tag{10}$$

The elastic orthogonal virtual rotation of the $n$th link has been given by Equation 11.

$$\delta\Pi^{S_n}=\begin{bmatrix}1 & 0 & w_n'/(e_n+1)\\ 0 & \cos\gamma_n & r_n\sin\gamma_n/(e_n+1)\\ 0 & -\sin\gamma_n & r_n\cos\gamma_n/(e_n+1)\end{bmatrix}\begin{bmatrix}\delta\gamma_n\\ \delta\beta_n\\ \delta\alpha_n\end{bmatrix}$$

$$=\begin{bmatrix}1\\0\\0\end{bmatrix}\delta\gamma_n+C_n\begin{bmatrix}\delta u_n'\\ \delta v_n'\\ \delta w_n'\end{bmatrix}. \tag{11}$$

Equation 12 is the elastic angular velocity of the $n$th link. Based on the Kirchhoff kinetic analogy [1], the elastic normalized curvature of the $n$th link, i.e. Equation 13, has been obtained from Equation 12. It should be noted that normalized and real curvatures arise by differentiation, with respect to $ds_n$ and $(1+e_n)ds_n$, relating to un-deformed and deformed situations, respectively. The elastic angular acceleration and variation of the elastic normalized curvature of the $n$th link are required to be derived from Equations 12 and 13, respectively.

$$\Omega^{S_n}=\left[1 \quad 0 \quad 0\right]^T\dot{\gamma}_n+C_n\left[\dot{u}_n' \quad \dot{v}_n' \quad \dot{w}_n'\right]^T, \tag{12}$$

$$\kappa^{S_n}=\left[1 \quad 0 \quad 0\right]^T\gamma_n'+C_n\left[u_n'' \quad v_n'' \quad w_n''\right]^T. \tag{13}$$

Considering Figures 1 and 5 and the apparent position of the representative point of the links' cross-section given by Equation 3, the exact elastic displacement field is given by Equation 14.

$$\Delta_n=\xi_n-\xi_n^0=\left[u_n \quad v_n \quad w_n\right]^T$$

$$+\underset{B_nS_n}{R}\left[0 \quad y_n \quad z_n\right]^T-\left[0 \quad y_n \quad z_n\right]^T. \tag{14}$$

One may obtain Equation 15. It should be noted that a beam has only one non-functional space variable, i.e. $s_n$.

$$\partial\Delta_n/\partial s_n=\left[u_n' \quad v_n' \quad w_n'\right]^T$$

$$+\underset{B_nS_n}{R}\left[(-y_n\kappa_{n_z}+z_n\kappa_{n_y}) \quad -z_n\kappa_{n_x} \quad y_n\kappa_{n_x}\right]^T. \tag{15}$$

The linear part of the Green-Lagrange geometric strain tensor is: $\varepsilon_{n_{ij}}=0.5\left(\partial\Delta_{n_i}/\partial s_{n_j}+\partial\Delta_{n_j}/\partial s_{n_i}\right)$, so the exact components of this strain are given by Equations 16.

$$\varepsilon_{n_{xx}}=u_n'+y_n\left[\frac{v_n'\kappa_{n_x}}{r_n}\sin\gamma_n-\frac{h_n}{1+e_n}\left(\kappa_{n_z}+\frac{w_n'\kappa_{n_x}}{r_n}\cos\gamma_n\right)\right]+z_n\left[\frac{v_n'\kappa_{n_x}}{r_n}\cos\gamma_n+\frac{h_n}{1+e_n}\left(\kappa_{n_y}+\frac{w_n'\kappa_{n_x}}{r_n}\sin\gamma_n\right)\right],$$

$$\varepsilon_{n_{xy}}=\frac{v_n'}{2}-\frac{y_n}{2}\left[\frac{h_n\kappa_{n_x}}{r_n}\sin\gamma_n+\frac{v_n'}{1+e_n}\left(\kappa_{n_z}+\frac{w_n'\kappa_{n_x}}{r_n}\cos\gamma_n\right)\right]-\frac{z_n}{2}\left[\frac{h_n\kappa_{n_x}}{r_n}\cos\gamma_n-\frac{v_n'}{1+e_n}\left(\kappa_{n_y}+\frac{w_n'\kappa_{n_x}}{r_n}\sin\gamma_n\right)\right],$$

$$\varepsilon_{n_{xz}}=\frac{w_n'}{2}+\frac{y_n}{2}\left[\frac{-w_n'\kappa_{n_z}+r_n\kappa_{n_x}\cos\gamma_n}{1+e_n}\right]+\frac{z_n}{2}\left[\frac{w_n'\kappa_{n_y}-r_n\kappa_{n_x}\sin\gamma_n}{1+e_n}\right],$$

$$\varepsilon_{n_{yy}}=\varepsilon_{n_{zz}}=\varepsilon_{n_{yz}}=0. \tag{16}$$

### Revolute Joints

As shown in Figures 1 and 2, the 3rd axes of $F_{E_{0J}}$, $F_{B_{nJ}}$ and $F_{E_{nJ}}$ are considered as the axes of the revolute joints. The joint variable of the $n$th revolute joint of the robot has been shown by angle $\Theta_n$. The joint variable, $\Theta_n$, is a given function of time in inverse dynamics, unlike forward dynamics. Driving /damping torques are not considered in the revolute joints because the non-conservative forces/moments have been ignored in the present article.

### Beginning Frame of the Links

The beginning frame of each link, i.e. $F_{B_n}$, has been illustrated by Figures 1-5. The kinematical parameters of the beginning frame of the 1st link are derived, based on the kinematical parameters of the mobile base. Orientation of the beginning frame of the 1st link is described by the rotation transformation matrix of Equation 17. Angular velocity/acceleration and orthogonal virtual rotation of the beginning frame of the 1st link are required to be obtained.

$$\underset{B_1I}{R} = \underset{B_1B_{1_J}}{R}\ \underset{B_{1_J}E_{0_J}}{R}\ \underset{E_{0_J}B_0}{R}\ \underset{B_0I}{R}. \tag{17}$$

The position of the beginning frame of the 1st link is given by Equation 18. The virtual displacement, velocity and acceleration of the beginning frame of the 1st link are required to be obtained.

$$b_1 = b_0 + \underset{IB_0}{R}\, D_0. \tag{18}$$

The kinematical parameters of the beginning frame of the $(n+1)$st link are derived based on the kinematical parameters of the beginning frame of the $n$st link, while $1 \leq n \leq N-1$. Orientation of the beginning frame of the links is recursively described by the rotation transformation matrix of Equation 19. Angular velocity/acceleration and orthogonal virtual rotation of the beginning frame of the links are required to be obtained.

$$\underset{B_{n+1}I}{R} = \underset{B_{n+1}B_{n+1_J}}{R}\ \underset{B_{n+1_J}E_{n_J}}{R}\ \underset{E_{n_J}E_n}{R}\ \underset{E_nB_n}{R}\ \underset{B_nI}{R}. \tag{19}$$

The position of the beginning frame of the links is given by Equation 20. The virtual displacement, velocity and acceleration of the beginning frame of the links are also required to be obtained.

$$b_{n+1} = b_n + \underset{IB_n}{R}\, D_n. \tag{20}$$

### End-Effector

The end-effector is shown in Figure 1. Kinematical parameters of the end-effector are obtained, based on the kinematical parameters of the beginning frame of the last link. Orientation of the end-effector is described by the rotation transformation matrix of Equation 21.

$$\underset{E_NI}{R} = \underset{E_NB_N}{R}\ \underset{B_NI}{R}. \tag{21}$$

The position of the end-effector is given by Equations 22.

$$b_{N+1} = b_N + \underset{IB_N}{R}\, D_N. \tag{22}$$

Traditionally, the pure kinematical robotic problem, within which the pose (position and orientation) of the end-effector is found in terms of the joint variables, is referred to as forward kinematics. The inverse problem, within which the joint variables are found in terms of the pose of the end-effector, is referred to as inverse kinematics. These problems are solved independent of the laws of motion.

Considering Equations 17-22 in mobile and/or flexible-link robots, unlike fixed-based rigid-link robots, determining the pose of the end-effector in terms of joint variables, and vice-versa is not a pure kinematical or geometrical problem since it is dependent upon the laws of motion and thus kinematics cannot be solved regardless of kinetics. Determination of the pose of the end-effector needs elastic and flying DoF and the time history and activation sequence of the desired joint variables, further than the final values of joint variables. As a result, in mobile and/or flexible-link robots, new terminologies, namely forward/inverse kinetics, are suggested to be used instead of the terms forward/inverse kinematics. It should be noted that the terms forward/inverse kinematics are only meaningful in fixed-based rigid-link robots.

## DYNAMICS

Hamilton's principle for a mobile robot containing $N$ long spatially flexible links is shown by Equation 23. It should be noted that non-conservative forces/moments which evidently include the driving torques of the revolute joints are assumed to be zero.

$$\int_0^t \left\{ \delta T_0 - \delta U_0^g + \sum_{n=1}^{N} \left( \delta T_n - \delta U_n^g - \delta U_n^e \right) \right\} dt = 0. \tag{23}$$

### Variation of Elastic Potential Energy of the Links

Each link as an isotropic linearly elastic medium has two independent elastic coefficients being used in the stress-strain law. Stress components are obtained in accordance with Hook's law. Variation of the elastic potential energy of the $n$th link is derived from Equation 24 within which the stresses and strains, i.e. Equation 16, have been substituted. At the first stage, the variation of elastic potential energy arises in terms of the variations of the spatial derivatives of the elastic DoF, namely $\delta u_n'$, $\delta v_n'$, $\delta w_n'$, $\delta \gamma_n$, $\delta \gamma_n'$, $\delta u_n''$, $\delta v_n''$ and $\delta w_n''$.

$$\delta U_n^e = \int_0^{L_n} \int_{A_n} \{ \tau_{n_{xx}} \delta \varepsilon_{n_{xx}} + 2\tau_{n_{xy}} \delta \varepsilon_{n_{xy}} + 2\tau_{n_{xz}} \delta \varepsilon_{n_{xz}} \}\, dA_n ds_n. \tag{24}$$

Integration by part identities shown by Equations 25 and 26 has been applied to derive the variation of the elastic potential energy of the $n$th link in terms of the variations of the elastic DoF, namely $\delta u_n$, $\delta v_n$, $\delta w_n$ and $\delta\gamma_n$ [4].

$$\int F\delta u' ds = F\delta u - \int F'\delta u ds, \tag{25}$$

$$\int F\delta u'' ds = F\delta u' - F'\delta u + \int F''\delta u ds. \tag{26}$$

**Variation of Gravitational Potential Energy**

Variation of the gravitational potential energy of the mobile base is given by Equation 27.

$$\delta U_0^g = m_0 g \begin{bmatrix} 0 & 0 & 1 \end{bmatrix} \delta b_0 = m_0 g \delta z_0. \tag{27}$$

Considering the fact that $S_n$ is the center of the cross-sectional area of the link, the variation of the gravitational potential energy of the $n$th link is obtained from the following equation:

$$\begin{aligned} \delta U_n^g &= \int_0^{L_n} \int_{A_n} \left\{ \begin{bmatrix} 0 & 0 & 1 \end{bmatrix} \delta \eta_n \right\} g \rho_n dA_n ds_n \\ &= g\rho_n A_n \begin{bmatrix} 0 & 0 & 1 \end{bmatrix} \int_0^{L_n} \left\{ \delta b_n + \underset{IB_n}{R}\, \delta d_n \right. \\ &\quad \left. - \underset{IB_n}{R}\, \widetilde{d_n} \delta\pi^{B_n} \right\} ds_n. \end{aligned} \tag{28}$$

**Variation of Kinetic Energy**

Time integration of the variation of kinetic energy is the negative of the virtual work of inertia forces/moments. Time integration of the variation of kinetic energy of the mobile base is obtained from the following equation:

$$\begin{aligned} \int_0^t \delta T_0 dt = \int_0^t \Bigg\{ &-m_0 \left[ \underset{I}{a}^{B_0} \right]^T \delta b_0 \\ &- \left( \left[ \dot{\omega}^{B_0} \right]^T [I_0] - \left[ \omega^{B_0} \right]^T [I_0] \widetilde{\omega}^{B_0} \right) \delta\pi^{B_0} \Bigg\} dt. \end{aligned} \tag{29}$$

Time integration of the variation of kinetic energy of the $n$th link is obtained from Equation 30.

$$\int_0^t \delta T_n dt = \int_0^t \int_0^{L_n} \int_{A_n} \left\{ -\rho_n \begin{bmatrix} \overset{\sigma_n}{a} \\ {\scriptstyle B_n} \end{bmatrix}^T \left[ \underset{B_n I}{R}\, \delta\eta_n \right] \right\} dA_n ds_n dt. \tag{30}$$

Using integration by part identity shown by Equation 25, and by considering the fact that $S_n$ is the center of the cross-sectional area of the link, Equation 30 has been simplified to Equation 31.

$$\begin{aligned} \int_0^t \delta T_n dt = -\rho_n \int_0^t \Bigg\{ \int_0^{L_n} \Bigg\{ &\varphi_n^T \underset{B_n I}{R}\, \delta b_n \\ &+ \left[ \varphi_n^R \underset{S_n B_n}{R} - \varphi_n^T \widetilde{d_n} \right] \delta\pi^{B_n} + \varphi_n^R \begin{bmatrix} 1 \\ 0 \\ 0 \end{bmatrix} \delta\gamma_n \\ &+ \left[ \varphi_n^T - \left( \varphi_n^R C_n \right)' \right] \begin{bmatrix} \delta u_n \\ \delta v_n \\ \delta w_n \end{bmatrix} \Bigg\} ds_n \\ &+ \varphi_n^R C_n \begin{bmatrix} \delta u_n \\ \delta v_n \\ \delta w_n \end{bmatrix} \Bigg|_{s_n = 0}^{s_n = L_n} \Bigg\} dt. \end{aligned} \tag{31}$$

**General Structure**

Using some agent variables, namely $A_j^i$, $\bar{A}_j^i$, $B_j^i$ and $\bar{B}_j^i$, the general structure of the dynamic model of a mobile robot with $N$ long spatially flexible links and $N$ revolute joints has been obtained from Equation 23. The Hamilton principle in terms of $A_j^i$, $\bar{A}_j^i$, $B_j^i$ and $\bar{B}_j^i$ has been exposed by Equation 32. Fifty agent variables appear in the dynamic model when $N = 2$. In Appendix A, the agent variables having sizes dependent on $N$, i.e. $\{A_1^n, A_2^n, \cdots, A_6^n; 0 < n \le N\}$, $\{A_{5k+2}^n; 0 < k \le n \le N\}$ and $\{A_{5k+3}^n, \cdots, A_{5k+6}^n, \bar{A}_{5k+4}^n, \cdots, \bar{A}_{5k+6}^n; 1 < k+1 \le n \le N\}$, are determined for $N = 2$. In Appendix B, the agent variables having sizes independent of $N$, i.e. $\{A_{5n+3}^n, \cdots, A_{5n+6}^n, B_{5n+3}^n, \cdots, B_{5n+6}^n, \bar{B}_{5n+4}^n, \cdots, \bar{B}_{5n+6}^n; 0 < n \le N\}$ and $\{A_1^0, \cdots, A_6^0\}$, are determined for any $N$.

$$\begin{aligned} \int_0^t \Bigg\{ &\left[ A_1^0 + \sum_{n=1}^N \int_0^{L_n} A_1^n ds_n \right] \delta x_0 \\ &+ \left[ A_2^0 + \sum_{n=1}^N \int_0^{L_n} A_2^n ds_n \right] \delta y_0 \\ &+ \left[ A_3^0 + \sum_{n=1}^N \int_0^{L_n} A_3^n ds_n \right] \delta z_0 \\ &+ \left[ A_4^0 + \sum_{n=1}^N \int_0^{L_n} A_4^n ds_n \right] \delta\pi_{0_x} \\ &+ \left[ A_5^0 + \sum_{n=1}^N \int_0^{L_n} A_5^n ds_n \right] \delta\pi_{0_y} \end{aligned}$$

$$+\left[A_6^0+\sum_{n=1}^{N}\int_0^{L_n}A_6^n ds_n\right]\delta\pi_{0_z}$$
$$+\sum_{k=1}^{N}\left[\sum_{n=k}^{N}\int_0^{L_n}A_{5k+2}^n ds_n\right]\delta\Theta_k$$
$$+\sum_{n=1}^{N}\int_0^{L_n}(A_{5n+3}^n\delta\gamma_n+A_{5n+4}^n\delta u_n+A_{5n+5}^n\delta v_n$$
$$+A_{5n+6}^n\delta w_n)ds_n-\sum_{n=1}^{N}(B_{5n+3}^n\delta\gamma_n+B_{5n+4}^n\delta u_n$$
$$+B_{5n+5}^n\delta v_n+B_{5n+6}^n\delta w_n+\bar{B}_{5n+4}^n\delta u_n'$$
$$+\bar{B}_{5n+5}^n\delta v_n'+\bar{B}_{5n+6}^n\delta w_n')\Big|_{s_n=0}$$
$$+(B_{5N+3}^N\delta\gamma_N+B_{5N+4}^N\delta u_N+B_{5N+5}^N\delta v_N$$
$$+B_{5N+6}^N\delta w_N+\bar{B}_{5N+4}^N\delta u_N'+\bar{B}_{5N+5}^N\delta v_N'$$
$$+\bar{B}_{5N+6}^N\delta w_N')\Big|_{s_N=L_N}$$
$$+\sum_{k=1}^{N-1}\left(\left[B_{5k+3}^k+\sum_{n=k+1}^{N}\int_0^{L_n}A_{5k+3}^n ds_n\right]\delta\gamma_k\right.$$
$$+\left[B_{5k+4}^k+\sum_{n=k+1}^{N}\int_0^{L_n}A_{5k+4}^n ds_n\right]\delta u_k$$
$$+\left[B_{5k+5}^k+\sum_{n=k+1}^{N}\int_0^{L_n}A_{5k+5}^n ds_n\right]\delta v_k$$
$$+\left[B_{5k+6}^k+\sum_{n=k+1}^{N}\int_0^{L_n}A_{5k+6}^n ds_n\right]\delta w_k$$
$$+\left[\bar{B}_{5k+4}^k+\sum_{n=k+1}^{N}\int_0^{L_n}\bar{A}_{5k+4}^n ds_n\right]\delta u_k'$$
$$+\left[\bar{B}_{5k+5}^k+\sum_{n=k+1}^{N}\int_0^{L_n}\bar{A}_{5k+5}^n ds_n\right]\delta v_k'$$
$$\left.+\left[\bar{B}_{5k+6}^k+\sum_{n=k+1}^{N}\int_0^{L_n}\bar{A}_{5k+6}^n ds_n\right]\delta w_k'\right)\Big|_{s_k=L_k}\Bigg\}dt=0. \tag{32}$$

Since there is not any contact constraint and the flying and elastic DoF are independent coordinates, the general structure of the dynamic model of the robot has been easily obtained by equating the coefficients of the variation of the coordinates within Equation 32 with zero. As a result, the motions equations, i.e. Equations 33, are found as a set of $5N+6$ nonlinear coupled partial differential equations under the influence of the boundary conditions shown by Equations 34.

$$A_1^0+\sum_{n=1}^{N}\int_0^{L_n}A_1^n ds_n=0,\qquad A_2^0+\sum_{n=1}^{N}\int_0^{L_n}A_2^n ds_n=0,$$
$$A_3^0+\sum_{n=1}^{N}\int_0^{L_n}A_3^n ds_n=0,\qquad A_4^0+\sum_{n=1}^{N}\int_0^{L_n}A_4^n ds_n=0,$$
$$A_5^0+\sum_{n=1}^{N}\int_0^{L_n}A_5^n ds_n=0,\qquad A_6^0+\sum_{n=1}^{N}\int_0^{L_n}A_6^n ds_n=0,$$
$$\sum_{n=k}^{N}\int_0^{L_n}A_{5k+2}^n ds_n=0,\qquad (k=1,2,\cdots,N),$$
$$A_{5n+3}^n=0,\qquad A_{5n+4}^n=0,\qquad A_{5n+5}^n=0,$$
$$A_{5n+6}^n=0;\qquad (n=1,2,\cdots,N). \tag{33}$$

Equations 33 are coupled, but it can be recognized that the first six equations of Equations 33 correspond to the flying movement of the robot; the 7th equations correspond to the $N$ angular movements of the revolute joints and the 8th, 9th, 10th and 11th equations, respectively, correspond to the twisting, axial and two spatial bending movements of the $N$ long spatially flexible links.

$$\{(B_{5n+3}^n=0 \text{ or } \gamma_n=0)\ \&\ (B_{5n+4}^n=0 \text{ or } u_n=0)$$
$$\&\ (B_{5n+5}^n=0 \text{ or } v_n=0)\ \&\ (B_{5n+6}^n=0 \text{ or } w_n=0)$$
$$\&\ (\bar{B}_{5n+4}^n=0 \text{ or } u_n'=0)\ \&\ (\bar{B}_{5n+5}^n=0 \text{ or } v_n'=0)$$
$$\&\ (\bar{B}_{5n+6}^n=0 \text{ or } w_n'=0)\}\ |_{s_n=0},$$
$$1\leq n\leq N,$$
$$\{(B_{5N+3}^N=0 \text{ or } \gamma_N=0)\ \&\ (B_{5N+4}^N=0 \text{ or } u_N=0)$$
$$\&\ (B_{5N+5}^N=0 \text{ or } v_N=0)\ \&\ (B_{5N+6}^N=0 \text{ or } w_N=0)$$
$$\&\ (\bar{B}_{5N+4}^N=0 \text{ or } u_N'=0)\ \&\ (\bar{B}_{5N+5}^N=0 \text{ or } v_N'=0)$$
$$\&(\bar{B}_{5N+6}^N=0 \text{ or } w_N'=0)\}\ |_{s_N=L_N},$$

$$\left\{ \left( B^k_{5k+3} + \sum_{n=k+1}^{N} \int_0^{L_n} A^n_{5k+3} ds_n = 0 \text{ or } \gamma_k = 0 \right) \right.$$

$$\& \left( B^k_{5k+4} + \sum_{n=k+1}^{N} \int_0^{L_n} A^n_{5k+4} ds_n = 0 \text{ or } u_k = 0 \right)$$

$$\& \left( B^k_{5k+5} + \sum_{n=k+1}^{N} \int_0^{L_n} A^n_{5k+5} ds_n = 0 \text{ or } v_k = 0 \right)$$

$$\& \left( B^k_{5k+6} + \sum_{n=k+1}^{N} \int_0^{L_n} A^n_{5k+6} ds_n = 0 \text{ or } w_k = 0 \right)$$

$$\& \left( \bar{B}^k_{5k+4} + \sum_{n=k+1}^{N} \int_0^{L_n} \bar{A}^n_{5k+4} ds_n = 0 \text{ or } u'_k = 0 \right)$$

$$\& \left( \bar{B}^k_{5k+5} + \sum_{n=k+1}^{N} \int_0^{L_n} \bar{A}^n_{5k+5} ds_n = 0 \text{ or } v'_k = 0 \right)$$

$$\left. \& \left( \bar{B}^k_{5k+6} + \sum_{n=k+1}^{N} \int_0^{L_n} \bar{A}^n_{5k+6} ds_n = 0 \text{ or } w'_k = 0 \right) \right\} \Bigg|_{s_k = L_k},$$

$$1 \leq k \leq N-1. \tag{34}$$

It should be noted that $B^n_{5n+3}$ and $B^k_{5k+3} + \sum_{n=k+1}^{N} \int_0^{L_n} A^n_{5k+3} ds_n$ are the twisting moment about the 1st axis; $B^n_{5n+4}$ and $B^k_{5k+4} + \sum_{n=k+1}^{N} \int_0^{L_n} A^n_{5k+4} ds_n$ are the axial force along the 1st axis; $B^n_{5n+5}$ and $B^n_{5n+6}$, and also $B^k_{5k+5} + \sum_{n=k+1}^{N} \int_0^{L_n} A^n_{5k+5} ds_n$ and $B^k_{5k+6} + \sum_{n=k+1}^{N} \int_0^{L_n} A^n_{5k+6} ds_n$ are the transverse shear forces along the 2nd and 3rd axes; and $\bar{B}^n_{5n+5}$ and $\bar{B}^n_{5n+6}$, and also $\bar{B}^k_{5k+5} + \sum_{n=k+1}^{N} \int_0^{L_n} \bar{A}^n_{5k+5} ds_n$ and $\bar{B}^k_{5k+6} + \sum_{n=k+1}^{N} \int_0^{L_n} \bar{A}^n_{5k+6} ds_n$ are the bending moments about the 3rd and 2nd axes of the cross-sectional frame of the $n$th link.

## CONCLUSIONS

Two outstanding novelties of the present article arise from the large elastic orientation of the links and from the dynamic model itself, regardless of how flexible the links are. This dynamic model is composed of the motion equations, links' section loads and boundary conditions. It is a unified dynamic model for flying and/or fixed-base robots and/or multiple pendulums with rigid and/or flexible links serially connected by revolute joints, one flying rigid body and long and/or short fully-enhanced and/or short enhanced and/or short generalized nonlinear 3D and/or 2D Euler-Bernoulli beams with a flying and/or a fixed support. This unified dynamic model has been referred to as the general structure of the dynamic model in this article and with the aid of some agent variable has been achieved for a spatial mobile robot with $N$ spatially flexible links and $N$ revolute joints. It is composed of a set of $5N + 6$ nonlinear coupled partial differential motion equations, i.e. Equations 33, under the influence of the boundary conditions, i.e. Equations 34. The base of the robot is an unconstraint rigid body in space. The links are long 3D Euler-Bernoulli beams undergoing tension-compression, torsion and two spatial bendings, while elastic orientation is considerable and the nonlinear part of the geometric Green-Lagrange strain is ignored. The driving and damping torque is not considered in the revolute joints, due to the fact that the non-conservative forces and moments have been ignored in this article. If the non-conservative forces and moments are considered, the general structure of the dynamic model will not change, but a few exciting and/or damping terms will arise within the agent variables.

The agent variables of Appendix B have sizes independent of $N$ and can create the dynamic model of a nonlinear 3D long Euler-Bernoulli beam having fixed/flying support and considerable elastic orientation. It contains twisting moment, axial force, transverse shear forces, bending moments and four coupled nonlinear partial differential motion equations governing the twisting, axial and two spatial bending deformations of the beam, under the influence of the boundary conditions. The agent variables of Appendix A have sizes dependent upon $N$ and, therefore, are presented only for $N = 2$ in this article. Fifty agent variables have appeared in the dynamic model when $N = 2$.

### Verification of the Dynamic Model

- It might be verified that, when the elastic orientation is neglected, the dynamic model of each link remains more accurate than a nonlinear 3D Euler-Bernoulli beam [1] within which the elastic orientation is in fact negligible. When the revolute joints are changed to rigid joints, the mobile base is mass-less, $N = 1$, and the links' elastic orientation is negligible, then the dynamic model of fully-enhanced/enhanced/generalized nonlinear 3D Euler-Bernoulli beams, having a fixed/flying support, can be obtained [2,3,4]. When the support is fixed and the elastic orientation and the nonlinear terms are ignored, the famous four decoupled motion equations of a linear 3D short Euler-Bernoulli beam with a fixed support are obtained as Equations 35-38 [2-3,13].

$$2J[(G/\rho_n)\gamma_n'' - \ddot{\gamma}_n] = 0, \tag{35}$$

$$A_n[(E/\rho_n)u_n'' - \ddot{u}_n] = 0, \tag{36}$$

$$-\ddot{v}_n - (EJ/\rho_n A_n)v_n'''' = 0, \tag{37}$$

$$-\ddot{w}_n - (EJ/\rho_n A_n)w_n'''' = g. \tag{38}$$

- It might be verified that, when the links' flexibility is ignored, the dynamic model is reduced to a set of $N+6$ nonlinear coupled ordinary differential equations of motion. This verification has proved to be valid for a double pendulum in [13] (while the base is fixed and $N=2$) and, for a flying rigid prism with a circular or square cross-section under gravitational force in [2] (while the revolute joints are changed to rigid joints, and the base becomes mass-less and $N=1$).
- It might be verified that, when the elastic orientation is negligible and $N=2$, sixteen coupled nonlinear partial differential motion equations and the boundary conditions of a flying manipulator having two highly flexible links are obtained [13].

In the following, unless otherwise specified, the index condition, $1 \le n \le N$, is valid.

## NOMENCLATURE

| | |
|---|---|
| $A_n$ | cross-sectional area in the plane constructed by the 2nd and 3rd axes of $F_{S_n}$ |
| $A_j^i, \bar{A}_j^i, B_j^i, \bar{B}_j^i$ | agent variables |
| ${}_I a^{B_0}$ | acceleration of $B_0$ being projected onto $F_1$; $[\ddot{x}_0\ \ddot{y}_0\ \ddot{z}_0]^T$ |
| ${}_I a^{B_n}$ | acceleration of $B_n$ being projected onto $F_I$ |
| ${}_I a^{E_N}$ | acceleration of $E_N$ being projected onto $F_I$; acceleration of the end-effector |
| ${}_{B_n} a^{\sigma_n}$ | acceleration of $\sigma_n$ being projected onto $F_{B_n}$ |
| $B_0$ | mass center of the mobile base |
| $B_n$ | area center of the cross-section at the beginning of the $n$th link; $S_n$ when $s_n = 0$ |
| $b_0$ | position of $B_0$ from $I$ being projected onto $F_I$; $\begin{bmatrix} x_0 & y_0 & z_0 \end{bmatrix}^T$ |
| $b_n$ | position of $B_n$ from $I$ projected onto $F_I$ |
| $C_n$ | agent variable; $\begin{bmatrix} -\frac{w_n' v_n'}{r_n^2(e_n+1)} & \frac{w_n' h_n}{r_n^2(e_n+1)} & 0 \\ \frac{-v_n'(e_n+1)\sin\gamma_n + w_n' h_n \cos\gamma_n}{r_n(e_n+1)^2} & \frac{h_n(e_n+1)\sin\gamma_n + v_n' w_n' \cos\gamma_n}{r_n(e_n+1)^2} & -\frac{r_n\cos\gamma_n}{(e_n+1)^2} \\ \frac{-v_n'(e_n+1)\cos\gamma_n - w_n' h_n \sin\gamma_n}{r_n(e_n+1)^2} & \frac{h_n(e_n+1)\cos\gamma_n - v_n' w_n' \sin\gamma_n}{r_n(e_n+1)^2} & \frac{r_n\sin\gamma_n}{(e_n+1)^2} \end{bmatrix}$ |
| $D_0$ | constant position of $E_0$ from $B_0$ being projected onto $F_{B_0}$ |
| $D_n$ | position of $E_n$ from $B_n$ being projected onto $F_{S_n^0}$; $d_n$ when $s_n = L_n$ |
| $d_n$ | elastic displacement vector of $S_n$ from $B_n$ being projected onto $F_{S_n^0}$; $\begin{bmatrix} u_n(s_n,t)+s_n & v_n(s_n,t) & w_n(s_n,t) \end{bmatrix}^T$ |
| $E$ | modulus of elasticity; Young's modulus |
| $E_0$ | a point on the mobile rigid base being coincided with $B_1$ |
| $E_n$ | area center of the cross-section at the end of the $n$th link; $S_n$ when $s_n = L_n$ |
| $E_N$ | origin of the frame of the end-effector |
| $e_n$ | centerline axial strain of the $n$th link; $\sqrt{r_n^2 + w_n'^2} - 1$ |
| $F_{B_0}$ | principal body frame of the mobile rigid base having $B_0$ as origin |
| $F_{B_n}$ | beginning frame of the $n$th link having $B_n$ as origin; $F_{S_n}$ when $s_n = 0$ |
| $F_{B_{nJ}}$ | beginning joint frame of the $n$th link having $B_n$ as origin |
| $F_{E_{0J}}$ | joint frame of the mobile rigid base having $E_0$ as origin |
| $F_{E_n}$ | end frame of the $n$th link having $E_n$ as origin; $F_{S_n}$ when $s_n = L_n$ |
| $F_{E_{nJ}}$ | end joint frame of the $n$th link having $E_n$ as origin, $1 \le n \le (N-1)$ |
| $F_{E_N}$ | the frame of the end-effector having $E_N$ as origin; $F_{E_n}$ when $n = N$ |
| $F_I$ | inertial reference frame assumed to have a 3rd axis in the opposite direction of gravity |
| $F_{S_n}, F_{S_n^0}$ | cross-sectional frames of the $n$th link after and before elastic deformation having $S_n$ abd $S_n^0$, respectively, as origin |
| $G$ | shear modulus of elasticity; modulus of rigidity |
| $g$ | magnitude of the gravitational acceleration |
| $h_n$ | agent variable; $1 + u_n'$ |

$[I_0]$ — rotary inertia tensor of the mobile rigid base being projected onto $F_{B_0}$; $\mathrm{diag}(I_{0_{xx}}, I_{0_{yy}}, I_{0_{zz}})$

$I_{3\times 3}$ — identity matrix; $\mathrm{diag}(1,1,1)$

$[J_{S_n}]$ — rotary cross-sectional area tensor of the $n$th link being projected onto $F_{S_n}$: $-\int_{A_n} \widetilde{p_n}\widetilde{p_n} dA_n$

$J, 2J$ — moment of cross-sectional area of the $n$th link about the 2nd or 3rd axis of $F_{S_n}$ and polar moment of cross-sectional area of the $n$th link about the 1st axis of $F_{S_n}$

$L_n$ — undeformed length of the $n$th link

$m_0$ — mass of the mobile rigid base

$N$ — number of revolute joints and/or number of links being straight before elastic deformation

$p_n$ — constant position of $\sigma_n$ from $S_n$ being projected onto $F_{S_n}$; $\begin{bmatrix} 0 & y_n & z_n \end{bmatrix}^T$

$\widetilde{p_n}$ — $\begin{bmatrix} 0 & -z_n & y_n \\ z_n & 0 & 0 \\ -y_n & 0 & 0 \end{bmatrix}$

$\underset{B_0 I}{R}$ — Rotation transformation matrix projecting a vector from $F_I$ onto $F_{B_0}$ being a function of $\theta_0$, $\phi_0$ and $\psi_0$;

$$\begin{bmatrix} 1 & 0 & 0 \\ 0 & \cos\psi_0 & \sin\psi_0 \\ 0 & -\sin\psi_0 & \cos\psi_0 \end{bmatrix} \begin{bmatrix} \cos\phi_0 & 0 & -\sin\phi_0 \\ 0 & 1 & 0 \\ \sin\phi_0 & 0 & \cos\phi_0 \end{bmatrix} \begin{bmatrix} \cos\theta_0 & \sin\theta_0 & 0 \\ -\sin\theta_0 & \cos\theta_0 & 0 \\ 0 & 0 & 1 \end{bmatrix}$$

$\underset{B_n I}{R}$ — rotation transformation matrix projecting a vector from $F_I$ onto $F_{B_n}$

$\underset{B_{nJ} B_n}{R}$ — constant rotation transformation matrix projecting a vector from $F_{B_n}$ onto $F_{B_{nJ}}$

$\underset{B_{nJ} E_{n-1J}}{R}$ — rotation transformation matrix projecting a vector from $F_{E_{n-1J}}$ onto $F_{B_{nJ}}$ being a function of $\Theta_n$

$\underset{E_n B_n}{R}$ — rotation transformation matrix projecting a vector from $F_{B_n}$ onto $F_{E_n}$; $\underset{S_n B_n}{R}$ when $s_n = L_n$

$\underset{E_{0J} B_0}{R}$ — constant rotation transformation matrix projecting a vector from $F_{B_0}$ onto $F_{E_{0J}}$

$\underset{E_{nJ} E_n}{R}$ — constant rotation transformation matrix projecting a vector from $F_{E_n}$ onto $F_{E_{nJ}}$, $1 \le n \le (N-1)$

$\underset{E_N I}{R}$ — rotation transformation matrix projecting a vector from $F_I$ onto $F_{E_N}$ accounting for the end-effector orientation

$\underset{S_n B_n}{R}$ — elastic rotation transformation matrix projecting a vector from $F_{B_n}$ onto $F_{S_n}$ being a function of $\alpha_n$, $\beta_n$, $\gamma_n$ and/or $u'_n, v'_n, w'_n, \gamma_n$;

$$\begin{bmatrix} 1 & 0 & 0 \\ 0 & \cos\gamma_n & \sin\gamma_n \\ 0 & -\sin\gamma_n & \cos\gamma_n \end{bmatrix} \begin{bmatrix} \cos\beta_n & 0 & -\sin\beta_n \\ 0 & 1 & 0 \\ \sin\beta_n & 0 & \cos\beta_n \end{bmatrix} \begin{bmatrix} \cos\alpha_n & \sin\alpha_n & 0 \\ -\sin\alpha_n & \cos\alpha_n & 0 \\ 0 & 0 & 1 \end{bmatrix} =$$

$$\begin{bmatrix} h_n/(e_n+1) & v'_n/(e_n+1) & w'_n/(e_n+1) \\ -v'_n\cos\gamma_n/r_n - w'_n h_n \sin\gamma_n/[r_n(e_n+1)] & h_n\cos\gamma_n/r_n - w'_n v'_n \sin\gamma_n/[r_n(e_n+1)] & r_n\sin\gamma_n/(e_n+1) \\ v'_n\sin\gamma_n/r_n - w'_n h_n\cos\gamma_n/[r_n(e_n+1)] & -h_n\sin\gamma_n/r_n - w'_n v'_n\cos\gamma_n/[r_n(e_n+1)] & r_n\cos\gamma_n/(e_n+1) \end{bmatrix}$$

$r_n$ — agent variable; $\sqrt{h_n^2 + v_n'^2}$

$S_n, S_n^0$ — center of cross-sectional area of the $n$th link after and before elastic deformation

$s_n$ — non-functional variable of space denoting the distance of $S_n^0$ from $B_n$

$T_0, T_n$ — kinetic energy of the mobile rigid base and the $n$th link

$t$ — non-functional variable of time

$U_n^e$ — elastic potential energy of the $n$th link

$U_n^g$ — gravitational potential energy of the $n$th link

| | |
|---|---|
| $u_n$ | elastic axial deformation at $S_n$ along the 1st axis of $F_{S_n^0}$ being a function of $s_n$ and $t$ |
| $\underset{I}{V}^{B_0}$ | velocity of $B_0$ projected onto $F_I$; $\begin{bmatrix}\dot{x}_0 & \dot{y}_0 & \dot{z}_0\end{bmatrix}^T$ |
| $\underset{I}{V}^{B_n}$ | velocity of $B_n$ projected onto $F_I$ |
| $\underset{I}{V}^{E_N}$ | velocity of $E_N$ projected onto $F_I$; the velocity of the end-effector |
| $v_n$ | elastic bending deflection at $S_n$ along the 2nd axis of $F_{S_n^0}$ being a function of $s_n$ and $t$ |
| $w_n$ | elastic bending deflection at $S_n$ along the 3rd axis of $F_{S_n^0}$ being a function of $s_n$ and $t$ |
| $x_0, y_0, z_0$ | components of $b_0$ being functions of $t$ |
| $y_n, z_n$ | components of $p_n$ |
| $\alpha_n$ | so-called elastic bending rotation angle at $S_n$ about the 3rd axis of $F_{S_n^0}$ being a function of $u'_n, v'_n$ and eventually a function of $s_n$ and $t$ |
| $\beta_n$ | so-called elastic bending rotation angle at $S_n$ about the 2nd axis of the updated $F_{S_n^0}$ by $\alpha_n$ being a function of $u'_n, v'_n, w'_n$ and eventually a function of $s_n$ and $t$ |
| $\gamma_n$ | so-called elastic twisting angle at $S_n$ about the 1st axis of $F_{S_n}$ being a function of $s_n$ and $t$ |
| $\Delta_n$ | elastic displacement of $\sigma_n$ being projected onto $F_{S_n^0}$ |
| $\Delta u_n$, $\Delta v_n$, $\Delta w_n$, $\Delta s_n$ | growth of $u_n, v_n, w_n$ and $s_n$ |
| $\delta b_0$ | $\begin{bmatrix}\delta x_0 & \delta y_0 & \delta z_0\end{bmatrix}^T$ |
| $\delta d_n$ | $\begin{bmatrix}\delta u_n & \delta v_n & \delta w_n\end{bmatrix}^T$ |
| $\delta D_n$ | $\delta d_n$ when $s_n = L_n$ |
| $\delta\pi_{0_x}$, $\delta\pi_{0_y}$, $\delta\pi_{0_z}$ | components of $\delta\pi^{B_0}$ |
| $\delta\Pi_{n_x}$, $\delta\Pi_{n_y}$, $\delta\Pi_{n_z}$ | components of $\delta\Pi^{S_n}$ |
| $\delta\Pi^{E_n}$ | elastic orthogonal virtual rotation of $F_{E_n}$ relative to $F_{S_n^0}$ being projected onto $F_{E_n}$; $\delta\Pi^{S_n}$ when $s_n = L_n$ |
| $\delta\Pi^{S_n}$ | elastic orthogonal virtual rotation of $F_{S_n}$ relative to $F_{S_n^0}$ being projected onto $F_{S_n}$; $\begin{bmatrix}\delta\Pi_{n_x} & \delta\Pi_{n_y} & \delta\Pi_{n_z}\end{bmatrix}^T$ |
| $\delta\pi^{B_0}$ | orthogonal virtual rotation of $F_{B_0}$ being projected onto $F_{B_0}$; $\begin{bmatrix}\delta\pi_{0_x} & \delta\pi_{0_y} & \delta\pi_{0_z}\end{bmatrix}^T$ |
| $\delta\pi^{B_n}$ | orthogonal virtual rotation of $F_{B_n}$ being projected onto $F_{B_n}$ |
| $\delta\underset{S_n}{\pi}^{B_n}$ | projection of $\delta\pi^{B_n}$ onto $F_{S_n}$; $\underset{S_nB_n}{R}\,\delta\pi^{B_n}$ |
| $\delta\underset{S_n}{\widetilde{\pi}}^{B_n}$ | projection of $\delta\widetilde{\pi}^{B_n}$ onto $F_{S_n}$; $\underset{S_nB_n}{R}\,\delta\widetilde{\pi}^{B_n}\,\underset{B_nS_n}{R}$ |
| $\varepsilon_{n_{xx}}$, $\varepsilon_{n_{xy}}$, $\varepsilon_{n_{xz}}$, $\varepsilon_{n_{yy}}$, $\varepsilon_{n_{yz}}$, $\varepsilon_{n_{zz}}$ | exact components of the linear part of Green-Lagrange geometric strain in the $n$th link |
| $\eta_n$ | position of $\sigma_n$ from $I$ being projected onto $F_I$ |
| $\Theta_n$ | joint variable of the $n$th revolute joint |
| $\theta_0, \phi_0, \psi_0$ | euler angles corresponding to the orientation of the mobile rigid base about the 3rd axis of $F_I$, 2nd axis of the updated $F_I$ by $\theta_0$ and about the 1st axis of $F_{B_0}$ respectively being functions of $t$ |
| $\kappa^{E_n}$ | elastic normalized curvature of $F_{E_n}$ relative to $F_{B_n}$ being projected onto $F_{E_n}$; $\kappa^{S_n}$ when $s_n = L_n$ |
| $\kappa^{S_n}$ | elastic normalized curvature of $F_{S_n}$ relative to $F_{B_n}$ being projected onto $F_{S_n}$; $\begin{bmatrix}\kappa_{n_x} & \kappa_{n_y} & \kappa_{n_z}\end{bmatrix}^T$ |
| $\kappa_{n_x}$ | twisting component of $\kappa^{S_n}$ being about the 1st axis of $F_{S_n}$ |
| $\kappa_{n_y}, \kappa_{n_z}$ | bending components of $\kappa^{S_n}$ being about the 2nd and 3rd axes of $F_{S_n}$, respectively |
| $\lambda$ | Lame's elastic coefficient for isotropic beam |
| $\mu$ | Lame's elastic coefficient for isotropic beam; $G$ |
| $\nu$ | poisson's ratio |
| $\xi_n, \xi_n^0$ | position of $\sigma_n$ from $B_n$ being projected onto $F_{S_n^0}$ after and before elastic deformation |
| $\rho_n$ | density of the $n$th link |
| $\sigma_n$ | representative point in the cross-sectional area of the $n$th link |
| $\tau_{n_{xx}}$, $\tau_{n_{xy}}$, $\tau_{n_{xz}}$, $\tau_{n_{yy}}$, $\tau_{n_{yz}}$, $\tau_{n_{zz}}$ | components of stress in the $n$th link |
| $\varphi_n^T$ | agent variable; $A_n\left\{\left[\underset{I}{a}^{B_n}\right]^T \underset{IB_n}{R} + \ddot{d}_n^T - 2\dot{d}_n^T\widetilde{\omega}^{B_n} + d_n^T\left(\widetilde{\omega}^{B_n}\widetilde{\omega}^{B_n} - \dot{\widetilde{\omega}}^{B_n}\right)\right\}$ |
| $\varphi_n^R$ | agent variable; |

$$\left\{\left[\dot{\Omega}^{S_n}\right]^T + \left[\dot{\omega}^{B_n}\right]^T \underset{B_nS_n}{R}\right\}[J_{S_n}]$$
$$- \left[\Omega^{S_n}\right]^T [J_{S_n}]\,\widetilde{\Omega}^{S_n} +$$
$$\left[\omega^{B_n}\right]^T \underset{B_nS_n}{R}\left\{2J_{S_{n_p}}\widetilde{\Omega}^{S_n}\right.$$
$$\left.- [J_{S_n}]\left(2\widetilde{\Omega}^{S_n} + \underset{S_nB_n}{R}\,\widetilde{\omega}^{B_n}\,\underset{B_nS_n}{R}\right)\right\}$$

| | |
|---|---|
| $\Omega^{E_n}$ | elastic angular velocity of $F_{E_n}$ relative to $F_{S_n^0}$ being projected onto $F_{E_n}$; $\Omega^{S_n}$ when $s_n = L_n$ |
| $\Omega^{S_n}$ | elastic angular velocity of $F_{S_n}$ relative to $F_{S_n^0}$ being projected onto $F_{S_n}$; $\left[\Omega_{n_x} \quad \Omega_{n_y} \quad \Omega_{n_z}\right]^T$ |
| $\Omega^{\Theta_n}$ | angular velocity of the $n$th revolute joint; angular velocity of $F_{B_n}$ relative to $F_{E_{n-1}}$ or of $F_{B_{nJ}}$ relative to $F_{E_{n-1J}}$ being projected onto $F_{B_{nJ}}$ or $F_{E_{n-1J}}$; $\left[0 \quad 0 \quad \dot{\Theta}_n\right]^T$ |
| $\dot{\Omega}^{\Theta_n}$ | $\left[0 \quad 0 \quad \ddot{\Theta}_n\right]^T$ |
| $\widetilde{\Omega}^{\Theta_n}$ | $\begin{bmatrix} 0 & -1 & 0 \\ 1 & 0 & 0 \\ 0 & 0 & 0 \end{bmatrix} \dot{\Theta}_n$ |
| $\omega^{B_0}$ | angular velocity of the mobile rigid base being projected onto $F_{B_0}$ |
| $\omega^{B_n}$ | angular velocity of $F_{B_n}$ being projected onto $F_{B_n}$ |
| $\omega^{E_N}$ | angular velocity of $F_{E_N}$ being projected onto $F_{E_N}$; angular velocity of the end-effector |
| $\underset{S_n}{\omega}^{B_n}$ | projection of $\omega^{B_n}$ onto $F_{S_n}$; $\underset{S_nB_n}{R}\,\omega^{B_n}$ |
| $\underset{S_n}{\widetilde{\omega}}^{B_n}$ | projection of $\widetilde{\omega}^{B_n}$ onto $F_{S_n}$; $\underset{S_nB_n}{R}\,\widetilde{\omega}^{B_n}\,\underset{B_nS_n}{R}$ |
| $\dot{[\ ]}$ | partial differentiation with respect to $t$; $\frac{\partial}{\partial t}[\ ]$ |
| $[\quad_n]'$ | partial differentiation with respect to $s_n$; $\frac{\partial}{\partial S_n}[\ ]$ |

## REFERENCES


1. Nayfeh, A.H. and Pai, P.F., *Linear and Nonlinear Structural Mechanics*, Wiley Series in Nonlinear Science, John Wiley & Sons, Inc., Hoboken, New Jersey (2004).
2. Zohoor, H. and Khorsandijou, S.M. "Enhanced nonlinear 3D Euler-Bernoulli beam with flying support", *J. Nonlinear Dynamics*, **51**(1-2), pp. 217-230 (Jan. 2008).
3. Zohoor, H. and Khorsandijou, S.M. "Generalized nonlinear 3D Euler-Bernoulli beam", *Iranian Journal of Science & Technology, Transaction B, Engineering*, **32**(B1), pp. 1-12 (Feb. 2008).
4. Khorsandijou, S.M. "Nonlinear dynamic analysis of a spatial mobile flexible robot", PhD thesis, School of Mechanical Engineering, Sharif University of Technology (Feb. 2007).
5. Book, W.J. "Structural flexibility of motion systems in the space environment", *IEEE Transactions on Robotics and Automation, Special Issue on Space Robotics*, **9**(5), pp. 524-530 (Oct. 1993).
6. Putz, P. "Space robotics in europe: A survey", *Robotics and Autonomous Systems*, **23**(1-2), pp. 3-16 (March 1998).
7. Yang, K.J., Hong, K.S. and Matsuno, F. "Robust adaptive control of a cantilevered flexible structure with spatiotemporally varying coefficients and bounded disturbance", *JSME International Journal, Series C: Mechanical Systems, Machine Elements and Manufacturing*, **47**(3), pp. 812-822 (Sept. 2004).
8. Kakizaki, T., Deck, J.F. and Dubowsky, S. "Modeling the spatial dynamics of robotic manipulators with flexible links and joint clearances", *Flexible Mechanism, Dynamics, and Robot Trajectories*, American Society of Mechanical Engineers, Design Engineering Division (Publication) DE, **24**, pp. 343-350 (1990).
9. Modi, V.J., Karray, F. and Mah, H. "A composite control scheme for joint tracking and active vibration suppression of mobile flexible manipulator systems", *Acta Astronautica*, **36**(5), pp. 261-270 (1995).
10. Karray, F., Modi, V.J. and Chan, J.K. "Path planning with obstacle avoidance as applied to a class of space based flexible manipulators", *Acta Astronautica*, **37**, pp. 69-86 (1995).
11. Hiller, M. "Modelling, simulation and control design for large and heavy manipulators", *Robotics and Autonomous Systems*, **19**, pp. 167-177 (1996).
12. Korayem, M.H. and Ghariblu, H. "Analysis of wheeled mobile flexible manipulator dynamic motions with maximum load carrying capacities", *Robotics and Autonomous Systems*, **48**, pp. 63-76 (2004).
13. Zohoor, H., Khorsandijou, S.M. "Dynamic model of a flying manipulator with two highly flexible links", *J. Applied Mathematical Modelling*, **32**(10), pp. 2117-2132 (October 2008).
14. Sunada, W.H. and Dubowsky, S. "On the dynamic analysis and behavior of industrial robotic manipulators with elastic members", *Journal of Mechanisms, Transmissions, and Automation in Design*, **105**(1), pp. 42-51 (March 1983).
15. Book, W.J. "Recursive Lagrangian dynamics of flexible manipulator arms", *International Journal of Robotics Research*, **3**(3), pp. 87-101 (Fall 1984).
16. Cetinkunt, S., Siciliano, B. and Book, W.J. "Symbol modelling and dynamic analysis of flexible manipulators", *IEEE Conference: Proceedings of the 1986 IEEE*

*International Conference on Systems, Man, and Cybernetics*, Atlanta, GA, USA Sponsor: IEEE Systems, Man, & Cybernetics Soc., New York, NY, USA pp. 798-803 (1986).

17. Hastings, G.G. and Book, W.J. "Linear dynamic model for flexible robotic manipulators", *IEEE Control Systems Magazine*, **7**(1), pp. 61-64 (Feb. 1987).
18. Dubowsky, S., Deck, J.F. and Costello, H. "Dynamic modeling of flexible spatial machine systems with clearance connections", *Journal of Mechanisms, Transmissions, and Automation in Design*, **109**(1), pp. 87-94 (March 1987).
19. Siciliano, B. and Book, W.J. "Singular perturbation approach to control of lightweight flexible manipulators", *International Journal of Robotics Research*, **7**(4), pp. 79-90 (August 1988).
20. Cetinkunt, S. and Book, W.J. "Symbolic modeling and dynamic simulation of robotic manipulators with complaint links and joints", *Robotics and Computer-Integrated Manufacturing*, **5**(4), pp. 301-310 (1989).
21. Dubowsky, S. "Application of finite-element methods to dynamic analysis of flexible spatial and co-planar linkage systems, part 2, sponsor: National aeronautics and space administration", Washington DC (May 1989).
22. Book, W.J. "Modeling design, and control of flexible manipulator arms: A tutorial review", *Proceedings of the 29th IEEE Conference on Decision and Control*, Honolulu, Hawaii, pp. 500-506 (5-7 Dec. 1990).
23. Matsuno, F. and Yamamoto, K. "Dynamic hybrid position/force control of a two degree-of-freedom flexible manipulator", *Journal of Robotic Systems*, **11**(5), pp. 355-366 (July 1994).
24. Matsuno, F., Asano, T. and Sakawa, Y. "Modeling and quasi-static hybrid position/ force control of constrained planar two-link flexible manipulators", *IEEE Transactions on Robotics and Automation*, **10**(3), pp. 287-97 (June 1994).
25. Rocco, P. and Book, W.J. "Modelling for two-time scale force/position control of flexible robots", *Proceedings of the 1996 IEEE International Conference on Robotics and Automation*, pp. 1941-1946 (April 1996).
26. Bernzen, W., Riege, B. and Hartmann, S. "Modeling and model fitting of flexible robots-a multibody system toolkit approach", *Journal of Intelligent and Robotic Systems: Theory & Applications*, **22**(2), pp. 165-175 (June 1998).
27. Shi, Z.X., Fung, E.H.K. and Li, Y.C. "Dynamic modelling of a rigid-flexible manipulator for constrained motion task control", *Applied Mathematical Modelling*, **23**, pp. 509-525 (1999).
28. Chen, W. "Dynamic modeling of multi-link flexible robotic manipulators", *Computers and Structures*, **79**, pp. 183-195 (2001).
29. Siciliano, B. and Villani, L. "An inverse kinematics algorithm for interaction control of a flexible arm with a compliant surface", *Control Engineering Practice*, **9**, pp. 191-198 (2001).
30. Tan, T.H., Lee, H.P. and Leng, G.S.B. "Dynamic stability of a radially rotating beam subjected to base-excitation", *Comput. Methods Appl. Mech. Engrg.*, **146**, pp. 265-279 (1997).
31. Shi, P., McPhee, J. and Heppler, G.R. "A deformation field for Euler-Bernoulli beams with applications to flexible multibody dynamics", *Multibody System Dynamics*, **5**(1), pp. 79-104 (Feb. 2001).
32. Yang, J.B., Jiang, L.J. and Chen, D.C.H. "Dynamic modelling and control of a rotating Euler-Bernoulli beam", *Journal of Sound and Vibration*, **274**(3-5), pp. 863-75 (22 July 2004).
33. Zohoor, H. and Khorsandijou, S.M. and Abedinnasab, M.H. "Modified nonlinear 3D Euler Bernoulli beam theory", *JSME International Journal of System Design and Dynamics*, **2**(5), pp. 1170-1182 (2008).
34. Novozhilov, V.V., *Foundations of the Nonlinear Theory of Elasticity*, Unabridged Dover, 1999, Republication of the work published by Graylock Press Rochester, NY, pp. 198-217 (1953).
35. Green, A.E. and Laws, N. "Remarks on the theory of rods", *Journal of Elasticity*, **3**(3), pp. 179-184 (Sept. 1973).
36. Green, A.E., F.R.S., Naghdi, P.M. and Wenner, M.L. "On the theory of rods I: Derivations from the three-dimensional equations", *Proc. R. Soc. Lond. A.*, **337**, pp. 451-483 (1974).
37. Green, A.E., F.R.S., Naghdi, P.M. and Wenner, M.L. "On the theory of rods II: Developments by direct approach", *Proc. R. Soc. Lond. A.*, **337**, pp. 485-507 (1974).
38. Antman, S.S. "Kirchhoff's problem for nonlinearly elastic rods", *Quarterly of Applied Mathematics*, **XXII**(3), pp. 221-239 (Oct. 1974).
39. Whitman, A.B. and DeSilva, C.N. "An exact solution in a nonlinear theory of rods", *Journal of Elasticity*, **4**(4), pp. 265-280 (Dec. 1974).
40. Naghdi, P.M. and Rubin, M.B. "Constrained theories of rods", *Journal of Elasticity*, **14**(4), pp. 343-361 (Dec. 1984).
41. Steigmann, D.J. and Faulkner, M.G. "Variational theory for spatial rods", *Journal of Elasticity*, **33**, pp. 1-26 (1993).
42. O'Reilly, O.M. and Turcotte, J.S. "On the steady motions of a rotating elastic rod", *Transactions of the ASME*, **68**, pp. 766-771 (Sept. 2001).

## APPENDIX A

The agent variables, having sizes dependent on $N$, namely:

$$\left\{A_1^n, A_2^n, \cdots, A_6^n; 0 < n \leq N\right\},$$

$$\left\{A_{5k+2}^n; 0 < k \leq n \leq N\right\},$$

and:

$$\{A^n_{5k+3}, \cdots, A^n_{5k+6}, \bar{A}^n_{5k+4}, \cdots, \bar{A}^n_{5k+6};$$
$$1 < k+1 \leq n \leq N\},$$

are determined for $N = 2$, here, in Appendix A. The agent variables:

$$\{A^n_1, A^n_2, \cdots, A^n_6; 0 < n \leq N = 2\}$$

are given by Equations A1-A3:

$$\begin{aligned} \begin{bmatrix} A^n_1 & A^n_2 & A^n_3 \end{bmatrix} &= -\rho_n A_n \left\{ \left[\underset{I}{a}^{B_n}\right]^T + \widehat{\varphi}_n \underset{B_n I}{R} \right\} \\ &\quad - g\rho_n A_n \begin{bmatrix} 0 & 0 & 1 \end{bmatrix}; \\ n &= 1, \cdots, N, \end{aligned} \tag{A1}$$

$$\begin{aligned} \begin{bmatrix} A^1_4 & A^1_5 & A^1_6 \end{bmatrix} &= g\rho_1 A_1 \begin{bmatrix} 0 & 0 & 1 \end{bmatrix} \underset{IB_0}{R} \Big( \widetilde{D}_0 \\ &\quad + \underset{B_0B_1}{R}\, \widetilde{d}_1 \underset{B_1B_0}{R} \Big) - \rho_1 \Big\langle \varphi^R_1 \underset{S_1B_0}{R} \\ &\quad - A_1 \left\{ \left[\underset{I}{a}^{B_1}\right]^T \underset{IB_0}{R} + \widehat{\varphi}_1 \underset{B_1B_0}{R} \right\} \Big( \widetilde{D}_0 \\ &\quad + \underset{B_0B_1}{R}\, \widetilde{d}_1 \underset{B_1B_0}{R} \Big) \Big\rangle, \end{aligned} \tag{A2}$$

$$\begin{aligned} \begin{bmatrix} A^2_4 & A^2_5 & A^2_6 \end{bmatrix} &= -\rho_2 \Big\langle \varphi^R_2 \underset{S_2B_0}{R} \\ &\quad - A_2 \left\{ \left[\underset{I}{a}^{B_2}\right]^T \underset{IB_0}{R} + \widehat{\varphi}_2 \underset{B_2B_0}{R} \right\} \Big[ \widetilde{D}_0 \\ &\quad + \underset{B_0B_1}{R} \Big( \widetilde{D}_1 + \underset{B_1B_2}{R}\, \widetilde{d}_2 \underset{B_2B_1}{R} \Big) \underset{B_1B_0}{R} \Big] \Big\rangle \\ &\quad + g\rho_2 A_2 \begin{bmatrix} 0 & 0 & 1 \end{bmatrix} \underset{IB_0}{R} \Big[ \widetilde{D}_0 \\ &\quad + \underset{B_0B_1}{R} \Big( \widetilde{D}_1 + \underset{B_1B_2}{R}\, \widetilde{d}_2 \underset{B_2B_1}{R} \Big) \underset{B_1B_0}{R} \Big]. \end{aligned} \tag{A3}$$

The agent variables $\{A^n_{5k+2}; 0 < k \leq n \leq N = 2\}$ are given by Equations A4-A6:

$$\begin{aligned} A^1_7 &= -\rho_1 \Big\langle \varphi^R_1 \underset{S_1B_1}{R} - A_1 \Big( \left[\underset{I}{a}^{B_1}\right]^T \underset{IB_1}{R} \\ &\quad + \widehat{\varphi}_1 \Big) \widetilde{d}_1 \Big\rangle \underset{B_1B_{1_J}}{R} \begin{bmatrix} 0 & 0 & 1 \end{bmatrix}^T \\ &\quad + g\rho_1 A_1 \begin{bmatrix} 0 & 0 & 1 \end{bmatrix} \underset{IB_1}{R}\, \widetilde{d}_1 \underset{B_1B_{1_J}}{R} \begin{bmatrix} 0 & 0 & 1 \end{bmatrix}^T, \end{aligned} \tag{A4}$$

$$\begin{aligned} A^2_7 &= -\rho_2 \Big\langle \varphi^R_2 \underset{S_2B_1}{R} - A_2 \left\{ \left[\underset{I}{a}^{B_2}\right]^T \underset{IB_1}{R} + \widehat{\varphi}_2 \underset{B_2B_1}{R} \right\} \\ &\quad \Big( \widetilde{D}_1 + \underset{B_1B_2}{R}\, \widetilde{d}_2 \underset{B_2B_1}{R} \Big) \Big\rangle \underset{B_1B_{1_J}}{R} \\ &\quad \begin{bmatrix} 0 & 0 & 1 \end{bmatrix}^T + g\rho_2 A_2 \begin{bmatrix} 0 & 0 & 1 \end{bmatrix} \underset{IB_1}{R} \\ &\quad \Big( \widetilde{D}_1 + \underset{B_1B_2}{R}\, \widetilde{d}_2 \underset{B_2B_1}{R} \Big) \underset{B_1B_{1_J}}{R} \begin{bmatrix} 0 & 0 & 1 \end{bmatrix}^T, \end{aligned} \tag{A5}$$

$$\begin{aligned} A^2_{12} &= -\rho_2 \Big\langle \varphi^R_2 \underset{S_2B_2}{R} - A_2 \Big( \left[\underset{I}{a}^{B_2}\right]^T \underset{IB_2}{R} \\ &\quad + \widehat{\varphi}_2 \Big) \widetilde{d}_2 \Big\rangle \underset{B_2B_{2_J}}{R} \begin{bmatrix} 0 & 0 & 1 \end{bmatrix}^T \\ &\quad + g\rho_2 A_2 \begin{bmatrix} 0 & 0 & 1 \end{bmatrix} \underset{IB_2}{R}\, \widetilde{d}_2 \underset{B_2B_{2_J}}{R} \begin{bmatrix} 0 & 0 & 1 \end{bmatrix}^T. \end{aligned} \tag{A6}$$

The agent variables $\{A^n_{5k+3}, \cdots, A^n_{5k+6}, \bar{A}^n_{5k+4}, \cdots, \bar{A}^n_{5k+6};\ 1 < k+1 \leq n \leq N = 2\}$ are given by Equations A7-A9:

$$\begin{aligned} A^2_8 &= -\rho_2 \Big\langle \varphi^R_2 \underset{S_2E_1}{R} - A_2 \Big\{ \left[\underset{I}{a}^{B_2}\right]^T \underset{IE_1}{R} \\ &\quad + \widehat{\varphi}_2 \underset{B_2E_1}{R} \Big\} \underset{E_1B_2}{R}\, \widetilde{d}_2 \underset{B_2E_1}{R} \Big\rangle \begin{bmatrix} 1 & 0 & 0 \end{bmatrix}^T \\ &\quad + g\rho_2 A_2 \begin{bmatrix} 0 & 0 & 1 \end{bmatrix} \underset{IB_2}{R}\, \widetilde{d}_2 \underset{B_2E_1}{R} \begin{bmatrix} 1 & 0 & 0 \end{bmatrix}^T, \end{aligned} \tag{A7}$$

$$\begin{aligned} \begin{bmatrix} A^2_9 & A^2_{10} & A^2_{11} \end{bmatrix} &= -\rho_2 A_2 \left\{ \left[\underset{I}{a}^{B_2}\right]^T \underset{IB_1}{R} + \widehat{\varphi}_2 \underset{B_2B_1}{R} \right\} \\ &\quad - g\rho_2 A_2 \begin{bmatrix} 0 & 0 & 1 \end{bmatrix} \underset{IB_1}{R}, \end{aligned} \tag{A8}$$

$$\begin{aligned} \begin{bmatrix} \bar{A}^2_9 & \bar{A}^2_{10} & \bar{A}^2_{11} \end{bmatrix} &= -\rho_2 \Big\langle \varphi^R_2 \underset{S_2E_1}{R} - A_2 \Big\{ \left[\underset{I}{a}^{B_2}\right]^T \underset{IE_1}{R} \\ &\quad + \widehat{\varphi}_2 \underset{B_2E_1}{R} \Big\} \underset{E_1B_2}{R}\, \widetilde{d}_2 \underset{B_2E_1}{R} \Big\rangle C_1 \\ &\quad + g\rho_2 A_2 \begin{bmatrix} 0 & 0 & 1 \end{bmatrix} \underset{IB_2}{R}\, \widetilde{d}_2 \underset{B_2E_1}{R} C_1. \end{aligned} \tag{A9}$$

## APPENDIX B

Here, in Appendix B, the agent variables, having sizes independent of $N$, namely $[A^0_1, \cdots, A^0_6]$ and:

$$\{A^n_{5n+3},\cdots,A^n_{5n+6},B^n_{5n+3},\cdots,B^n_{5n+6},\bar{B}^n_{5n+4},\cdots,\bar{B}^n_{5n+6};0<n\leq N\},$$

are determined for any $N$. The agent variables:

$$\{A^0_1,\cdots,A^0_6\},$$

are given by Equation's B1 and B2:

$$\begin{bmatrix}A^0_1 & A^0_2 & A^0_3\end{bmatrix}=-m_0\begin{bmatrix}\ddot{x}_0 & \ddot{y}_0 & (\ddot{z}_0+g)\end{bmatrix}, \tag{B1}$$

$$\begin{bmatrix}A^0_4 & A^0_5 & A^0_6\end{bmatrix}^T=-[I_0]\dot{\omega}^{B_0}-\widetilde{\omega}^{B_0}[I_0]\omega^{B_0}. \tag{B2}$$

The agent variable corresponding to the equation of torsion, i.e. twisting deformation, of the $n$th link is given by Equation B3:

$$\begin{aligned}-A^n_{5n+3}=&+\rho_n\Bigg[\left[\left[\dot{\Omega}^{S_n}\right]^T[J_{S_n}]-\left[\Omega^{S_n}\right]^T[J_{S_n}]\widetilde{\Omega}^{S_n}\right.\\&-2\left[\omega^{B_n}\right]^T\underset{B_nS_n}{R}[J_{S_n}]\widetilde{\Omega}^{S_n}+2J_{S_{n_p}}\left[\omega^{B_n}\right]^T\underset{B_nS_n}{R}\widetilde{\Omega}^{S_n}\\&-\left[\omega^{B_n}\right]^T\underset{B_nS_n}{R}[J_{S_n}]\underset{S_nB_n}{R}\widetilde{\omega}^{B_n}\underset{B_nS_n}{R}\\&\left.+\left[\dot{\omega}^{B_n}\right]^T\underset{B_nS_n}{R}[J_{S_n}]\right]\begin{bmatrix}1 & 0 & 0\end{bmatrix}^T\\&-\Bigg\langle\frac{(1-\nu)EJ}{(1+\nu)(1-2\nu)}\frac{1}{r_n^2(1+e_n)^2}\{\kappa_{n_x}[v_n'^2(1+e_n)^2\\&+h_n^2w_n'^2]+h_nr_n[v_n'(1+e_n)(\kappa_{n_y}\cos\gamma_n\\&-\kappa_{n_z}\sin\gamma_n)+h_nw_n'(\kappa_{n_y}\sin\gamma_n+\kappa_{n_z}\cos\gamma_n)]]\}\\&+GJ\frac{1}{r_n^2(1+e_n)^2}\{\kappa_{n_x}[r_n^4+(1+e_n)^2h_n^2+v_n'^2w_n'^2]\\&+h_nr_n[(1+e_n)v_n'(\kappa_{n_z}\sin\gamma_n-\kappa_{n_y}\cos\gamma_n)\\&-h_nw_n'(\kappa_{n_y}\sin\gamma_n+\kappa_{n_z}\cos\gamma_n)]]\}\Bigg\rangle'\\&+\frac{(1-\nu)EJ}{(1+\nu)(1-2\nu)}\frac{h_n}{r_n^2(e_n+1)^4}\{\kappa_{n_x}[w_n'h_n[r_n^2w_n''\\&-w_n'(h_nu_n''+v_n'v_n'')]+(e_n+1)^2\{r_n[h_nw_n'(\kappa_{n_y}\cos\gamma_n\\&-\kappa_{n_z}\sin\gamma_n)-(e_n+1)v_n'(\kappa_{n_y}\sin\gamma_n+\kappa_{n_z}\cos\gamma_n)]\\&+v_n'(h_nv_n''-v_n'u_n'')\}]+r_nh_n\{(h_nv_n''\\&-v_n'u_n'')(e_n+1)(\kappa_{n_y}\cos\gamma_n-\kappa_{n_z}\sin\gamma_n)\\&+[r_n^2w_n''-w_n'(h_nu_n''+v_n'v_n'')](\kappa_{n_y}\sin\gamma_n+\kappa_{n_z}\cos\gamma_n)\}\}\\&+GJ\{-\frac{h_n\kappa_{n_x}}{r_n(1+e_n)}\Bigg[\frac{h_n}{1+e_n}w_n'(\kappa_{n_y}\cos\gamma_n\\&-\kappa_{n_z}\sin\gamma_n)-v_n'(\kappa_{n_y}\sin\gamma_n+\kappa_{n_z}\cos\gamma_n)\Bigg]\\&+\frac{1}{r_n^2(e_n+1)^4}[\kappa_{n_x}\{(-h_nv_n''+v_n'u_n'')(e_n+1)^2h_nv_n'\\&+\left[r_n^2w_n''-w_n'(h_nu_n''+v_n'v_n'')\right]w_n'[v_n'(e_n+1)-r_n^2]\}\\&+\{(e_n+1)(h_nv_n''-v_n'u_n'')(\kappa_{n_y}\cos\gamma_n-\kappa_{n_z}\sin\gamma_n)\\&+[r_n^2w_n''-w_n'(h_nu_n''+v_n'v_n'')](\kappa_{n_y}\sin\gamma_n+\kappa_{n_z}\cos\gamma_n)\}\\&\cdot(v_n'^2+w_n'^2)r_n]\}.\end{aligned}\tag{B3}$$

The agent variable corresponding to the equation of tension/compression, i.e. axial deformation of the $n$th link is given by Equation B4:

$$\begin{aligned}-A^n_{5n+4}=&+\rho_n\{A_n([\underset{I}{a}^{B_n}]^T\underset{IB_n}{R}+\ddot{d}_n^T-2\dot{d}_n^T\widetilde{\omega}^{B_n}\\&+d_n^T[\widetilde{\omega}^{B_n}\widetilde{\omega}^{B_n}-\dot{\widetilde{\omega}}^{B_n}])-\langle[[\dot{\Omega}^{S_n}]^T[J_{S_n}]\\&-[\Omega^{S_n}]^T[J_{S_n}]\widetilde{\Omega}^{S_n}-2[\omega^{B_n}]^T\underset{B_nS_n}{R}[J_{S_n}]\widetilde{\Omega}^{S_n}\\&+2J_{S_{n_p}}[\omega^{B_n}]^T\underset{B_nS_n}{R}\widetilde{\Omega}^{S_n}\\&-[\omega^{B_n}]^T\underset{B_nS_n}{R}[J_{S_n}]\underset{S_nB_n}{R}\widetilde{\omega}^{B_n}\underset{B_nS_n}{R}+\\&+[\dot{\omega}^{B_n}]^T\underset{B_nS_n}{R}[J_{S_n}]]C_n\rangle'\}\begin{bmatrix}1 & 0 & 0\end{bmatrix}^T\\&+\langle\frac{(1-\nu)EJ}{(1+\nu)(1-2\nu)}\frac{1}{r_n^4(e_n+1)^4}\{(\kappa_{n_y}\cos\gamma_n\\&-\kappa_{n_z}\sin\gamma_n)h_nr_nw_n'[r_n^2h_n^2-(e_n+1)^2v_n'^2]\\&-(\kappa_{n_y}\sin\gamma_n+\kappa_{n_z}\cos\gamma_n)h_n^2r_nv_n'(e_n+1)^3\\&-\kappa_{n_x}v_n'w_n'(e_n+1)[(e_n+1)^2v_n'^2+h_n^2w_n'^2]\}\\&+GJ\{\frac{-w_n'v_n'}{r_n^4(e_n+1)}\{h_n^2\kappa_{n_x}+\frac{v_n'}{1+e_n}[h_nr_n(\kappa_{n_z}\sin\gamma_n\\&-\kappa_{n_y}\cos\gamma_n)+\frac{v_n'w_n'}{1+e_n}[w_n'\kappa_{n_x}+r_n(\kappa_{n_y}\sin\gamma_n\\&+\kappa_{n_z}\cos\gamma_n)]]\}+\frac{1}{r_n(e_n+1)^4}[h_nw_n'(v_n'^2\end{aligned}$$

$$+ w_n'^2)(\kappa_{n_y}\cos\gamma_n - \kappa_{n_z}\sin\gamma_n)$$
$$- v_n'(e_n+1)[w_n' r_n \kappa_{n_x} + v_n'^2(\kappa_{n_y}\sin\gamma_n$$
$$+ \kappa_{n_z}\cos\gamma_n)]]\}\rangle'' + \langle\frac{(1-\nu)EA_n}{(1+\nu)(1-2\nu)}u_n'$$
$$+ \frac{(1-\nu)EJ}{(1+\nu)(1-2\nu)}\{+\frac{1}{r_n^2(1+e_n)}[v_n' r_n\kappa_{n_x}(\kappa_{n_y}\cos\gamma_n$$
$$- \kappa_{n_z}\sin\gamma_n) + \frac{h_n}{1+e_n}[w_n'^2\kappa_{n_x}^2 + r_n^2(\kappa_{n_y}^2 + \kappa_{n_z}^2)$$
$$+ 2r_n w_n'\kappa_{n_x}(\kappa_{n_y}\sin\gamma_n + \kappa_{n_z}\cos\gamma_n)]]$$
$$+ \frac{h_n\kappa_{n_x}}{r_n^4}\{-v_n'^2\kappa_{n_x} + \frac{h_n}{1+e_n}[v_n' r_n(\kappa_{n_z}\sin\gamma_n$$
$$- \kappa_{n_y}\cos\gamma_n) - \frac{h_n w_n'}{1+e_n}[w_n'\kappa_{n_x} + r_n(\kappa_{n_z}\cos\gamma_n$$
$$+ \kappa_{n_y}\sin\gamma_n)]]\} + \frac{h_n^2}{r_n^2(1+e_n)^3}[v_n' r_n\kappa_{n_x}(\kappa_{n_z}\sin\gamma_n$$
$$- \kappa_{n_y}\cos\gamma_n) - \frac{h_n}{1+e_n}[w_n'^2\kappa_{n_x}^2 + r_n^2(\kappa_{n_z}^2 + \kappa_{n_y}^2)$$
$$+ 2w_n' r_n\kappa_{n_x}(\kappa_{n_y}\sin\gamma_n + \kappa_{n_z}\cos\gamma_n)]]$$
$$+ \frac{w_n'}{r_n^6(e_n+1)^3}\{v_n'^2\kappa_{n_x} + \frac{h_n}{1+e_n}[v_n' r_n(\kappa_{n_y}\cos\gamma_n$$
$$- \kappa_{n_z}\sin\gamma_n) + \frac{h_n w_n'}{1+e_n}[w_n'\kappa_{n_x} + r_n(\kappa_{n_y}\sin\gamma_n$$
$$+ \kappa_{n_z}\cos\gamma_n)]]\} \cdot \Big\{[2(e_n+1)^2 + r_n^2]h_n v_n' u_n''$$
$$+ [(e_n+1)^2 v_n'^2 - h_n^2[(e_n+1)^2 + r_n^2]]v_n''\Big\}$$
$$+ \frac{h_n}{r_n^4(e_n+1)^5}\{[(2r_n^2 + w_n'^2)h_n v_n' u_n'' + (v_n'^4 - h_n^4$$
$$+ w_n'^2 v_n'^2)v_n'']h_n[r_n(\kappa_{n_z}\cos\gamma_n + \kappa_{n_y}\sin\gamma_n) + w_n'\kappa_{n_x}]$$
$$+ [(v_n'^4 - 2h_n^4 - h_n^2 v_n'^2 + w_n'^2 v_n'^2)w_n' u_n''$$
$$- (3r_n^2 + w_n'^2)h_n w_n' v_n' v_n'' + (r_n^2 - w_n'^2)h_n r_n^2 w_n'']$$
$$\cdot [v_n'\kappa_{n_x} + \frac{h_n}{1+e_n}r_n(\kappa_{n_y}\cos\gamma_n - \kappa_{n_z}\sin\gamma_n)]]\}$$
$$+ GJ\{\frac{\kappa_{n_x}}{r_n^2}[h_n\kappa_{n_x} + \frac{v_n'}{1+e_n}r_n(\kappa_{n_z}\sin\gamma_n$$
$$- \kappa_{n_y}\cos\gamma_n)] + \frac{h_n\kappa_{n_x}}{r_n^4}\{-h_n^2\kappa_{n_x}$$
$$- \frac{v_n'}{1+e_n}[h_n r_n(\kappa_{n_z}\sin\gamma_n - \kappa_{n_y}\cos\gamma_n)$$
$$+ \frac{v_n' w_n'}{1+e_n}[w_n'\kappa_{n_x} + r_n(\kappa_{n_y}\sin\gamma_n + \kappa_{n_z}\cos\gamma_n)]]\}$$
$$+ \frac{h_n\kappa_{n_x}}{r_n(1+e_n)^2}[r_n\kappa_{n_x} - w_n'(\kappa_{n_y}\sin\gamma_n + \kappa_{n_z}\cos\gamma_n)]$$
$$+ \frac{h_n v_n'}{r_n^2(1+e_n)^3}[h_n r_n\kappa_{n_x}(\kappa_{n_y}\cos\gamma_n - \kappa_{n_z}\sin\gamma_n)$$
$$- \frac{v_n'}{1+e_n}[w_n'^2\kappa_{n_x}^2 + r_n^2(\kappa_{n_y}^2 + \kappa_{n_z}^2)$$
$$+ 2w_n' r_n\kappa_{n_x}(\kappa_{n_y}\sin\gamma_n + \kappa_{n_z}\cos\gamma_n)]]$$
$$+ \frac{h_n}{(1+e_n)^4}[r_n^2\kappa_{n_x}^2 + w_n'^2(\kappa_{n_y}^2 + \kappa_{n_z}^2)$$
$$- 2w_n' r_n\kappa_{n_x}(\kappa_{n_y}\sin\gamma_n + \kappa_{n_z}\cos\gamma_n)]$$
$$+ \frac{w_n'}{r_n^6(e_n+1)^3}\Big\{h_n^2\kappa_{n_x} + \frac{v_n'}{1+e_n}[h_n r_n(\kappa_{n_z}\sin\gamma_n$$
$$- \kappa_{n_y}\cos\gamma_n) + \frac{v_n' w_n'}{1+e_n}[w_n'\kappa_{n_x} + r_n(\kappa_{n_y}\sin\gamma_n$$
$$+ \kappa_{n_z}\cos\gamma_n)]]\} \cdot \{[2(e_n+1)^2 + r_n^2]h_n v_n' u_n''$$
$$+ [(e_n+1)^2 v_n'^2 - h_n^2[(e_n+1)^2 + r_n^2]]v_n''\}$$
$$+ \frac{w_n'}{r_n^3(e_n+1)^5}[r_n\kappa_{n_x} - w_n'(\kappa_{n_y}\sin\gamma_n$$
$$+ \kappa_{n_z}\cos\gamma_n)]\{[2(e_n+1)^2 + r_n^2]h_n v_n' u_n''$$
$$+ [(e_n+1)^2 v_n'^2 - h_n^2[(e_n+1)^2 + r_n^2]]v_n''\}$$
$$+ \frac{1}{r_n^4(e_n+1)^6}\{[(v_n'^4 - 2h_n^4 - h_n^2 v_n'^2 + w_n'^2 v_n'^2)w_n' u_n''$$
$$- (3r_n^2 + w_n'^2)h_n w_n' v_n' v_n'' + (r_n^2 - w_n'^2)h_n r_n^2 w_n'']$$
$$\cdot [(v_n'^2 + w_n'^2)r_n(\kappa_{n_y}\cos\gamma_n - \kappa_{n_z}\sin\gamma_n)$$
$$- h_n\kappa_{n_x}v_n'(e_n+1)] + [(2r_n^2 + w_n'^2)h_n v_n' u_n''$$
$$+ (v_n'^4 - h_n^4 + w_n'^2 v_n'^2)v_n''](e_n+1)[(v_n'^2 + w_n'^2)$$
$$\cdot r_n(\kappa_{n_y}\sin\gamma_n + \kappa_{n_z}\cos\gamma_n) - h_n^2 w_n'\kappa_{n_x}]]\}\}\rangle'. \qquad \text{(B4)}$$

The agent variables corresponding to the spatial bending equations of the $n$th link are, respectively, given by Equation's B5 and B6:

$$-A^n_{5n+5} = +\rho_n\{A_n([a^{B_n}_I]^T \underset{IB_n}{R} + \ddot{d}^T_n - 2\dot{d}^T_n\widetilde{\omega}^{B_n}$$

$$+ d^T_n[\widetilde{\omega}^{B_n}\widetilde{\omega}^{B_n} - \widetilde{\dot{\omega}}^{B_n}]) + \langle[[\dot{\Omega}^{S_n}]^T[J_{S_n}]$$

$$- [\Omega^{S_n}]^T[J_{S_n}]\widetilde{\Omega}^{S_n} - 2[\omega^{B_n}]^T \underset{B_nS_n}{R}[J_{S_n}]\widetilde{\Omega}^{S_n}$$

$$+ 2J_{S_{n_p}}[\omega^{B_n}]^T \underset{B_nS_n}{R} \widetilde{\Omega}^{S_n}$$

$$+ [\omega^{B_n}]^T \underset{B_nS_n}{R}[J_{S_n}] \underset{S_nB_n}{R} \widetilde{\omega}^{B_n} \underset{B_nS_n}{R}$$

$$+ [\dot{\omega}^{B_n}]^T \underset{B_nS_n}{R}[J_{S_n}]]C_n\rangle'\} \begin{bmatrix}0 & 1 & 0\end{bmatrix}^T$$

$$+ \langle\frac{(1-\nu)EJ}{(1+\nu)(1-2\nu)}\{\frac{w'_nh_n}{r^4_n(e_n+1)}\{v'^2_n\kappa_{n_x}$$

$$+ \frac{h_n}{1+e_n}[v'_nr_n(\kappa_{n_y}\cos\gamma_n - \kappa_{n_z}\sin\gamma_n)$$

$$+ \frac{h_nw'_n}{1+e_n}[w'_n\kappa_{n_x}+r_n(\kappa_{n_y}\sin\gamma_n+\kappa_{n_z}\cos\gamma_n)]]\}$$

$$+ \frac{h_n}{r^2_n(e_n+1)^3}[v'^2_nw'_n\kappa_{n_x}$$

$$+ \frac{h_n}{1+e_n}\{v'_nw'_nr_n(\kappa_{n_y}\cos\gamma_n - \kappa_{n_z}\sin\gamma_n)$$

$$+ (e_n+1)h_n[r_n(\kappa_{n_z}\cos\gamma_n + \kappa_{n_y}\sin\gamma_n)$$

$$+ w'_n\kappa_{n_x}]\}]\} + GJ\{\frac{w'_nh_n}{r^4_n(e_n+1)}\{h^2_n\kappa_{n_x}$$

$$+ \frac{v'_n}{1+e_n}[h_nr_n(\kappa_{n_z}\sin\gamma_n - \kappa_{n_y}\cos\gamma_n)$$

$$+ \frac{v'_nw'_n}{1+e_n}[w'_n\kappa_{n_x}+r_n(\kappa_{n_y}\sin\gamma_n+\kappa_{n_z}\cos\gamma_n)]]\}$$

$$+ \frac{}{r^2_n(1+e_n)^4}[r_nv'_nw'_n(\kappa_{n_y}\cos\gamma_n$$

$$-\kappa_{n_z}\sin\gamma_n)(v'^2_n+w'^2_n)+(e_n+1)h_nv'^2_nr_n(\kappa_{n_y}\sin\gamma_n$$

$$+ \kappa_{n_z}\cos\gamma_n)]\}\rangle'' + \langle GA_nv'_n$$

$$+\frac{(1-\nu)EJ}{(1+\nu)(1-2\nu)}\{\frac{\kappa_{n_x}}{r^2_n}[v'_n\kappa_{n_x}+\frac{h_nr_n}{1+e_n}(\kappa_{n_y}\cos\gamma_n$$

$$- \kappa_{n_z}\sin\gamma_n)] + \frac{v'_n\kappa_{n_x}}{r^4_n}\{-v'^2_n\kappa_{n_x}$$

$$+ \frac{h_n}{1+e_n}[v'_nr_n(\kappa_{n_z}\sin\gamma_n - \kappa_{n_y}\cos\gamma_n)$$

$$- \frac{h_nw'_n}{1+e_n}[w'_n\kappa_{n_x} + r_n(\kappa_{n_z}\cos\gamma_n + \kappa_{n_y}\sin\gamma_n)]]\}$$

$$+ \frac{h_nv'_n}{r^2_n(1+e_n)^3}[v'_nr_n\kappa_{n_x}(\kappa_{n_z}\sin\gamma_n - \kappa_{n_y}\cos\gamma_n)$$

$$- \frac{h_n}{1+e_n}[w'^2_n\kappa^2_{n_x} + r^2_n(\kappa^2_{n_z} + \kappa^2_{n_y})$$

$$+ 2w'_nr_n\kappa_{n_x}(\kappa_{n_y}\sin\gamma_n + \kappa_{n_z}\cos\gamma_n)]]$$

$$+ \frac{-1}{r^6_n(e_n+1)^3}w'_n\{v'^2_n\kappa_{n_x}+ \frac{h_n}{1+e_n}[v'_nr_n(\kappa_{n_y}\cos\gamma_n$$

$$- \kappa_{n_z}\sin\gamma_n) + \frac{h_nw'_n}{1+e_n}[w'_n\kappa_{n_x} + r_n(\kappa_{n_y}\sin\gamma_n$$

$$+ \kappa_{n_z}\cos\gamma_n)]]\} \cdot \{[2(e_n+1)^2 + r^2_n]h_nv'_nv''_n$$

$$+ [(e_n+1)^2h^2_n - v'^2_n[(e_n+1)^2 + r^2_n]]u''_n\}$$

$$+ \frac{h_n}{r^4_n(e_n+1)^5}\{[-(2r^2_n + w'^2_n)h_nv'_nv''_n + (v'^4_n - h^4_n$$

$$- w'^2_nh^2_n)u''_n]h_n[w'_n\kappa_{n_x}+r_n(\kappa_{n_y}\sin\gamma_n+\kappa_{n_z}\cos\gamma_n)]$$

$$+ [(h^4_n - 2v'^4_n - h^2_nv'^2_n + w'^2_nh^2_n)w'_nv''_n$$

$$- (3r^2_n + w'^2_n)h_nw'_nv'_nu''_n + (r^2_n - w'^2_n)v'_nr^2_nw''_n]$$

$$\cdot \left[v'_n\kappa_{n_x} + \frac{h_nr_n}{1+e_n}(\kappa_{n_y}\cos\gamma_n - \kappa_{n_z}\sin\gamma_n)\right]\}\}$$

$$+GJ\{\frac{1}{r^2_n(1+e_n)}[h_n\kappa_{n_x}r_n(\kappa_{n_z}\sin\gamma_n-\kappa_{n_y}\cos\gamma_n)$$

$$+ \frac{v'_n}{1+e_n}[r^2_n(\kappa^2_{n_y} + \kappa^2_{n_z}) + w'^2_n\kappa^2_{n_x}$$

$$+ 2w'_n\kappa_{n_x}r_n(\kappa_{n_y}\sin\gamma_n + \kappa_{n_z}\cos\gamma_n)]] + \frac{v'_n\kappa_{n_x}}{r^4_n}\{$$

$$- h^2_n\kappa_{n_x} - \frac{v'_n}{1+e_n}[h_nr_n(\kappa_{n_z}\sin\gamma_n - \kappa_{n_y}\cos\gamma_n)$$

$$+ \frac{v'_nw'_n}{1+e_n}[w'_n\kappa_{n_x} + r_n(\kappa_{n_y}\sin\gamma_n + \kappa_{n_z}\cos\gamma_n)]]\}$$

$$+ \frac{v'_n\kappa_{n_x}}{r_n(1+e_n)^2}[r_n\kappa_{n_x} - w'_n(\kappa_{n_y}\sin\gamma_n + \kappa_{n_z}\cos\gamma_n)]$$

$$+ \frac{v'^2_n}{r^2_n(1+e_n)^3}[h_nr_n\kappa_{n_x}(\kappa_{n_y}\cos\gamma_n - \kappa_{n_z}\sin\gamma_n)$$

$$- \frac{v'_n}{1+e_n}[w'^2_n\kappa^2_{n_x} + r^2_n(\kappa^2_{n_y} + \kappa^2_{n_z})$$

$$+ 2w'_n r_n \kappa_{n_x}(\kappa_{n_y} \sin\gamma_n + \kappa_{n_z} \cos\gamma_n)]]$$

$$+ \frac{v'_n}{(1+e_n)^4}[r_n^2 \kappa_{n_x}^2 + w_n'^2(\kappa_{n_y}^2 + \kappa_{n_z}^2)$$

$$- 2w'_n r_n \kappa_{n_x}(\kappa_{n_y} \sin\gamma_n + \kappa_{n_z} \cos\gamma_n)] + \{[2(e_n+1)^2$$

$$+ r_n^2]h_n v'_n v''_n + [(e_n+1)^2 h_n^2 - v_n'^2[(e_n+1)^2$$

$$+ r_n^2]]u''_n\}\{\frac{-w'_n}{r_n^3(e_n+1)^5}[r_n \kappa_{n_x} - w'_n(\kappa_{n_y} \sin\gamma_n$$

$$+ \kappa_{n_z} \cos\gamma_n)] + \frac{-w'_n}{r_n^6(e_n+1)^3}\{h_n^2 \kappa_{n_x}$$

$$+ \frac{v'_n}{1+e_n}[h_n r_n(\kappa_{n_z} \sin\gamma_n - \kappa_{n_y} \cos\gamma_n)$$

$$+ \frac{v'_n w'_n}{1+e_n}[w'_n \kappa_{n_x} + r_n(\kappa_{n_y} \sin\gamma_n + \kappa_{n_z} \cos\gamma_n)]]\}\}$$

$$+ \{\frac{v'_n}{r_n^4(e_n+1)^5}[-h_n \kappa_{n_x} \cos\gamma_n + \frac{v'_n}{1+e_n}(r_n \kappa_{n_y}$$

$$+ w'_n \kappa_{n_x} \sin\gamma_n)] + \frac{w'_n}{r_n^3(e_n+1)^6}(w'_n \kappa_{n_y} - r_n \kappa_{n_x} \sin\gamma_n)\}$$

$$\cdot \{[(h_n^4 - 2v_n'^4 - h_n^2 v_n'^2 + w_n'^2 h_n^2)w'_n v''_n$$

$$- (3r_n^2 + w_n'^2)h_n w'_n v'_n u''_n + (r_n^2 - w_n'^2)v'_n r_n^2 w''_n] \cos\gamma_n$$

$$+ [-(2r_n^2 + w_n'^2)h_n v'_n v''_n + (v_n'^4 - h_n^4$$

$$- w_n'^2 h_n^2)u''_n](e_n+1) \sin\gamma_n\}$$

$$+ \frac{1}{r_n^3(e_n+1)^5}\{\frac{v'_n}{r_n}[h_n \kappa_{n_x} \sin\gamma_n + \frac{v'_n}{1+e_n}(r_n \kappa_{n_z}$$

$$+ w'_n \kappa_{n_x} \cos\gamma_n)] + \frac{w'_n}{e_n+1}(w'_n \kappa_{n_z} - r_n \kappa_{n_x} \cos\gamma_n)\}$$

$$\cdot \{-[(h_n^4 - 2v_n'^4 - h_n^2 v_n'^2 + w_n'^2 h_n^2)w'_n v''_n$$

$$- (3r_n^2 + w_n'^2)h_n w'_n v'_n u''_n + (r_n^2 - w_n'^2)v'_n r_n^2 w''_n] \sin\gamma_n$$

$$+ [-(2r_n^2 + w_n'^2)h_n v'_n v''_n + (v_n'^4 - h_n^4$$

$$- w_n'^2 h_n^2)u''_n](e_n+1) \cos\gamma_n\}\}\rangle', \qquad \text{(B5)}$$

$$-A^n_{5n+6} = +\rho_n\{A_n(\left[a_I^{B_n}\right]^T \underset{IB_n}{R} + \ddot{d}_n^T - 2\dot{d}_n^T \widetilde{\omega}^{B_n}$$

$$+ d_n^T \left[\widetilde{\omega}^{B_n}\widetilde{\omega}^{B_n} - \dot{\widetilde{\omega}}^{B_n}\right]) - \langle[\left[\dot{\Omega}^{S_n}\right]^T [J_{S_n}]$$

$$- \left[\Omega^{S_n}\right]^T [J_{S_n}]\, \widetilde{\Omega}^{S_n} - 2\left[\omega^{B_n}\right]^T \underset{B_nS_n}{R} [J_{S_n}]\, \widetilde{\Omega}^{S_n}$$

$$+ 2J_{S_{n_p}} \left[\omega^{B_n}\right]^T \underset{B_nS_n}{R}\, \widetilde{\Omega}^{S_n}$$

$$+ \left[\omega^{B_n}\right]^T \underset{B_nS_n}{R} [J_{S_n}] \underset{S_nB_n}{R}\, \widetilde{\omega}^{B_n} \underset{B_nS_n}{R}$$

$$+ \left[\dot{\omega}^{B_n}\right]^T \underset{B_nS_n}{R} [J_{S_n}]]C_n\rangle'\} \begin{bmatrix}0 & 0 & 1\end{bmatrix}^T$$

$$+ \langle\frac{(1-\nu)EJ}{(1+\nu)(1-2\nu)}\frac{h_n}{(e_n+1)^3}[-v'_n \kappa_{n_x}$$

$$+ \frac{h_n r_n}{1+e_n}(\kappa_{n_z} \sin\gamma_n - \kappa_{n_y} \cos\gamma_n)]$$

$$+ GJ\{\frac{v'_n}{(e_n+1)^3}h_n \kappa_{n_x} + \frac{r_n}{(e_n+1)^4}(\kappa_{n_z} \sin\gamma_n$$

$$- \kappa_{n_y} \cos\gamma_n)(v_n'^2 + w_n'^2)\}\rangle'' + \langle GA_n w'_n$$

$$+ \frac{(1-\nu)EJ}{(1+\nu)(1-2\nu)}\{\frac{h_n^2 \kappa_{n_x}}{r_n^2(1+e_n)^2}[w'_n \kappa_{n_x}$$

$$+ r_n(\kappa_{n_y} \sin\gamma_n + \kappa_{n_z} \cos\gamma_n)]$$

$$+ \frac{h_n w'_n}{r_n^2(1+e_n)^3}[v'_n r_n \kappa_{n_x}(\kappa_{n_z} \sin\gamma_n - \kappa_{n_y} \cos\gamma_n)$$

$$- \frac{h_n}{1+e_n}[w_n'^2 \kappa_{n_x}^2 + r_n^2(\kappa_{n_z}^2 + \kappa_{n_y}^2)$$

$$+ 2w'_n r_n \kappa_{n_x}(\kappa_{n_y} \sin\gamma_n + \kappa_{n_z} \cos\gamma_n)]]$$

$$+ \frac{1}{r_n^2(e_n+1)^3}(h_n v''_n - v'_n u''_n)\{v_n'^2 \kappa_{n_x}$$

$$+ \frac{h_n}{1+e_n}[v'_n r_n(\kappa_{n_y} \cos\gamma_n - \kappa_{n_z} \sin\gamma_n)$$

$$+ \frac{h_n w'_n}{1+e_n}[w'_n \kappa_{n_x} + r_n(\kappa_{n_y} \sin\gamma_n + \kappa_{n_z} \cos\gamma_n)]]\}$$

$$+ \frac{h_n}{r_n^2(e_n+1)^5}\{[(r_n^2 - w_n'^2)(h_n u''_n + v'_n v''_n)$$

$$+ 2r_n^2 w'_n w''_n][v'_n \kappa_{n_x} + \frac{h_n r_n}{1+e_n}(\kappa_{n_y} \cos\gamma_n - \kappa_{n_z} \sin\gamma_n)]$$

$$+ (v'_n u''_n - h_n v''_n)h_n w'_n[w'_n \kappa_{n_x} + r_n(\kappa_{n_z} \cos\gamma_n$$

$$+ \kappa_{n_y} \sin\gamma_n)]]\}\} + GJ\{\frac{1}{(1+e_n)^2}[w'_n[\frac{v_n'^2}{r_n^2}\kappa_{n_x}^2$$

$$+ (\kappa_{n_y}^2 + \kappa_{n_z}^2)] - \frac{h_n^2 \kappa_{n_x}}{r_n}(\kappa_{n_y} \sin\gamma_n + \kappa_{n_z} \cos\gamma_n)]$$

$$+ \frac{v'_n w'_n}{r_n^2(1+e_n)^3}[h_n r_n \kappa_{n_x}(\kappa_{n_y} \cos\gamma_n - \kappa_{n_z} \sin\gamma_n)$$

$$
\begin{aligned}
&- \frac{v'_n}{1+e_n}[w'^2_n \kappa^2_{n_x} + r^2_n(\kappa^2_{n_y} + \kappa^2_{n_z})\\
&+ 2w'_n r_n \kappa_{n_x}(\kappa_{n_y} \sin\gamma_n + \kappa_{n_z} \cos\gamma_n)]]\\
&+ \frac{w'_n}{(1+e_n)^4}[r^2_n \kappa^2_{n_x} + w'^2_n(\kappa^2_{n_y} + \kappa^2_{n_z})\\
&- 2w'_n r_n \kappa_{n_x}(\kappa_{n_y} \sin\gamma_n + \kappa_{n_z} \cos\gamma_n)]\\
&+ \frac{1}{r^2_n(e_n+1)^3}(h_n v''_n - v'_n u''_n)\{h^2_n \kappa_{n_x}\\
&+ \frac{v'_n}{1+e_n}[h_n r_n(\kappa_{n_z} \sin\gamma_n - \kappa_{n_y} \cos\gamma_n)\\
&+ \frac{v'_n w'_n}{1+e_n}[w'_n \kappa_{n_x} + r_n(\kappa_{n_y} \sin\gamma_n + \kappa_{n_z} \cos\gamma_n)]]\}\\
&+ \frac{r_n}{(1+e_n)^5}(h_n v''_n - v'_n u''_n)[r_n \kappa_{n_x} - w'_n(\kappa_{n_y} \sin\gamma_n\\
&+ \kappa_{n_z} \cos\gamma_n)] + \frac{v'_n}{r^2_n(e_n+1)^5}\{[(r^2_n - w'^2_n)(h_n u''_n + v'_n v''_n)\\
&+ 2r^2_n w'_n w''_n][-h_n \kappa_{n_x} + \frac{v'_n}{1+e_n}(r_n \kappa_{n_y} \cos\gamma_n\\
&- r_n \kappa_{n_z} \sin\gamma_n)] + (v'_n u''_n - h_n v''_n)[r_n(\kappa_{n_y} \sin\gamma_n\\
&+ \kappa_{n_z} \cos\gamma_n) + w'_n \kappa_{n_x}]v'_n w'_n\}\\
&+ \frac{w'^2_n}{r_n(1+e_n)^6}\{[(r^2_n - w'^2_n)(h_n u''_n + v'_n v''_n)\\
&+ 2r^2_n w'_n w''_n](\kappa_{n_y} \cos\gamma_n - \kappa_{n_z} \sin\gamma_n)\\
&+ (v'_n u''_n - h_n v''_n)(e_n+1)[w'_n(\kappa_{n_z} \cos\gamma_n\\
&+ \kappa_{n_y} \sin\gamma_n) - r_n \kappa_{n_x}]\}\}\rangle'. \qquad \text{(B6)}
\end{aligned}
$$

The twisting moment about the 1st axis of the cross-sectional frame of the $n$th link is given by Equation B7:

$$
\begin{aligned}
-B^n_{5n+3} &= \frac{(1-\nu)EJ}{(1+\nu)(1-2\nu)} \frac{1}{r^2_n}\{v'^2_n \kappa_{n_x}\\
&+ \frac{h_n}{1+e_n}[v'_n r_n(\kappa_{n_y} \cos\gamma_n - \kappa_{n_z} \sin\gamma_n)\\
&+ \frac{h_n w'_n}{1+e_n}[w'_n \kappa_{n_x} + r_n(\kappa_{n_y} \sin\gamma_n + \kappa_{n_z} \cos\gamma_n)]]\}\\
&+ GJ\{\frac{1}{r^2_n}\{h^2_n \kappa_{n_x} + \frac{v'_n}{1+e_n}[h_n r_n(\kappa_{n_z} \sin\gamma_n\\
&- \kappa_{n_y} \cos\gamma_n) + \frac{v'_n w'_n}{1+e_n}[w'_n \kappa_{n_x} + r_n(\kappa_{n_y} \sin\gamma_n\\
&+ \kappa_{n_z} \cos\gamma_n)]]\} + \frac{r_n}{(1+e_n)^2}[r_n \kappa_{n_x}\\
&- w'_n(\kappa_{n_y} \sin\gamma_n + \kappa_{n_z} \cos\gamma_n)]\}. \qquad \text{(B7)}
\end{aligned}
$$

The axial force along the 1st axis of the cross-sectional frame of the $n$th link is given by Equation B8:

$$
\begin{aligned}
-B^n_{5n+4} &= +\rho_n[[\dot{\Omega}^{S_n}]^T[J_{S_n}] - [\Omega^{S_n}]^T[J_{S_n}]\widetilde{\Omega}^{S_n}\\
&- 2[\omega^{B_n}]^T \underset{B_n S_n}{R}[J_{S_n}]\widetilde{\Omega}^{S_n} + 2J_{S_{n_p}}[\omega^{B_n}]^T \underset{B_n S_n}{R}\widetilde{\Omega}^{S_n}\\
&+ [\omega^{B_n}]^T \underset{B_n S_n}{R}[J_{S_n}]\underset{S_n B_n}{R}\widetilde{\omega}^{B_n}\underset{B_n S_n}{R}\\
&+ [\dot{\omega}^{B_n}]^T \underset{B_n S_n}{R}[J_{S_n}]]C_n \begin{bmatrix}1 & 0 & 0\end{bmatrix}^T\\
&+ \langle\frac{(1-\nu)EJ}{(1+\nu)(1-2\nu)}\{\frac{-v'_n w'_n}{r^4_n(e_n+1)}\{v'^2_n \kappa_{n_x}\\
&+ \frac{h_n}{1+e_n}[v'_n r_n(\kappa_{n_y} \cos\gamma_n - \kappa_{n_z} \sin\gamma_n)\\
&+ \frac{h_n w'_n}{1+e_n}[w'_n \kappa_{n_x} + r_n(\kappa_{n_y} \sin\gamma_n + \kappa_{n_z} \cos\gamma_n)]]\}\\
&+ \frac{h_n}{r^2_n(e_n+1)^3}[h_n v'_n w'_n \kappa_{n_x}\\
&+ \frac{h_n}{1+e_n}\{h_n w'_n r_n(\kappa_{n_y} \cos\gamma_n - \kappa_{n_z} \sin\gamma_n)\\
&- (e_n+1)v'_n[r_n(\kappa_{n_y} \sin\gamma_n + \kappa_{n_z} \cos\gamma_n)\\
&+ w'_n \kappa_{n_x}]\}]\} + GJ\{\frac{-v'_n w'_n}{r^4_n(e_n+1)}\{h^2_n \kappa_{n_x}\\
&+ \frac{v'_n}{1+e_n}[h_n r_n(\kappa_{n_z} \sin\gamma_n - \kappa_{n_y} \cos\gamma_n)\\
&+ \frac{v'_n w'_n}{1+e_n}[w'_n \kappa_{n_x} + r_n(\kappa_{n_y} \sin\gamma_n + \kappa_{n_z} \cos\gamma_n)]]\}\\
&+ \frac{v'_n}{r^2_n(e_n+1)^3}[-w'_n h^2_n \kappa_{n_x}\\
&+ \frac{v'_n}{1+e_n}\{h_n w'_n r_n(\kappa_{n_y} \cos\gamma_n - \kappa_{n_z} \sin\gamma_n)\\
&-(e_n+1)v'_n[r_n(\kappa_{n_z} \cos\gamma_n + \kappa_{n_y} \sin\gamma_n) + w'_n \kappa_{n_x}]\}]\\
&+ \frac{w'_n}{r_n(e_n+1)^4}\{h_n w'^2_n(\kappa_{n_y} \cos\gamma_n - \kappa_{n_z} \sin\gamma_n)\\
&-(e_n+1)v'_n[w'_n(\kappa_{n_z} \cos\gamma_n + \kappa_{n_y} \sin\gamma_n) - r_n \kappa_{n_x}]\}
\end{aligned}
$$

$$+\frac{-w'_n v'_n}{r_n(e_n+1)^3}[r_n\kappa_{n_x}-w'_n(\kappa_{n_y}\sin\gamma_n$$

$$+\kappa_{n_z}\cos\gamma_n)]\}\})'+\frac{(1-\nu)EA_n}{(1+\nu)(1-2\nu)}u'_n$$

$$+\frac{(1-\nu)EJ}{(1+\nu)(1-2\nu)}\{+\frac{1}{r_n^2(1+e_n)}[v'_n r_n\kappa_{n_x}(\kappa_{n_y}\cos\gamma_n$$

$$-\kappa_{n_z}\sin\gamma_n)+\frac{h_n}{1+e_n}[w'^2_n\kappa^2_{n_x}+r_n^2(\kappa^2_{n_y}+\kappa^2_{n_z})$$

$$+2r_n w'_n\kappa_{n_x}(\kappa_{n_y}\sin\gamma_n+\kappa_{n_z}\cos\gamma_n)]]$$

$$+\frac{h_n\kappa_{n_x}}{r_n^4}\{-v'^2_n\kappa_{n_x}+\frac{h_n}{1+e_n}[v'_n r_n(\kappa_{n_z}\sin\gamma_n$$

$$-\kappa_{n_y}\cos\gamma_n)-\frac{h_n w'_n}{1+e_n}[w'_n\kappa_{n_x}+r_n(\kappa_{n_z}\cos\gamma_n$$

$$+\kappa_{n_y}\sin\gamma_n)]]\}+\frac{h_n^2}{r_n^2(1+e_n)^3}[v'_n r_n\kappa_{n_x}(\kappa_{n_z}\sin\gamma_n$$

$$-\kappa_{n_y}\cos\gamma_n)-\frac{h_n}{1+e_n}[w'^2_n\kappa^2_{n_x}+r_n^2(\kappa^2_{n_z}+\kappa^2_{n_y})$$

$$+2w'_n r_n\kappa_{n_x}(\kappa_{n_y}\sin\gamma_n+\kappa_{n_z}\cos\gamma_n)]]$$

$$+\frac{w'_n}{r_n^6(e_n+1)^3}\{v'^2_n\kappa_{n_x}+\frac{h_n}{1+e_n}[v'_n r_n(\kappa_{n_y}\cos\gamma_n$$

$$-\kappa_{n_z}\sin\gamma_n)+\frac{h_n w'_n}{1+e_n}[w'_n\kappa_{n_x}+r_n(\kappa_{n_y}\sin\gamma_n$$

$$+\kappa_{n_z}\cos\gamma_n)]]\}\cdot\{[2(e_n+1)^2+r_n^2]h_n v'_n u''_n$$

$$+[(e_n+1)^2 v'^2_n-h_n^2[(e_n+1)^2+r_n^2]]v''_n\}$$

$$+\frac{h_n}{r_n^4(e_n+1)^5}\{[(2r_n^2+w'^2_n)h_n v'_n u''_n+(v'^4_n-h_n^4$$

$$+w'^2_n v'^2_n)v''_n]h_n[r_n(\kappa_{n_z}\cos\gamma_n+\kappa_{n_y}\sin\gamma_n)$$

$$+w'_n\kappa_{n_x}]+[(v'^4_n-2h_n^4-h_n^2 v'^2_n+w'^2_n v'^2_n)w'_n u''_n$$

$$-(3r_n^2+w'^2_n)h_n w'_n v'_n v''_n+(r_n^2-w'^2_n)h_n r_n^2 w''_n]$$

$$\cdot[v'_n\kappa_{n_x}+\frac{h_n r_n}{1+e_n}(\kappa_{n_y}\cos\gamma_n-\kappa_{n_z}\sin\gamma_n)]\}\}$$

$$+GJ\{\frac{\kappa_{n_x}}{r_n^2}[h_n\kappa_{n_x}+\frac{v'_n}{1+e_n}r_n(\kappa_{n_z}\sin\gamma_n$$

$$-\kappa_{n_y}\cos\gamma_n)]+\frac{h_n\kappa_{n_x}}{r_n^4}\{-h_n^2\kappa_{n_x}$$

$$-\frac{v'_n}{1+e_n}[h_n r_n(\kappa_{n_z}\sin\gamma_n-\kappa_{n_y}\cos\gamma_n)$$

$$+\frac{v'_n w'_n}{1+e_n}[w'_n\kappa_{n_x}+r_n(\kappa_{n_y}\sin\gamma_n+\kappa_{n_z}\cos\gamma_n)]]\}$$

$$+\frac{h_n\kappa_{n_x}}{r_n(1+e_n)^2}[r_n\kappa_{n_x}-w'_n(\kappa_{n_y}\sin\gamma_n+\kappa_{n_z}\cos\gamma_n)]$$

$$+\frac{h_n v'_n}{r_n^2(1+e_n)^3}\Big[h_n r_n\kappa_{n_x}(\kappa_{n_y}\cos\gamma_n-\kappa_{n_z}\sin\gamma_n)$$

$$-\frac{v'_n}{1+e_n}[w'^2_n\kappa^2_{n_x}+r_n^2(\kappa^2_{n_y}+\kappa^2_{n_z})$$

$$+2w'_n r_n\kappa_{n_x}(\kappa_{n_y}\sin\gamma_n+\kappa_{n_z}\cos\gamma_n)]]$$

$$-\frac{h_n}{(1+e_n)^4}[r_n^2\kappa^2_{n_x}+w'^2_n(\kappa^2_{n_y}+\kappa^2_{n_z})$$

$$-2w'_n r_n\kappa_{n_x}(\kappa_{n_y}\sin\gamma_n+\kappa_{n_z}\cos\gamma_n)]$$

$$+\frac{w'_n}{r_n^6(e_n+1)^3}\{h_n^2\kappa_{n_x}+\frac{v'_n}{1+e_n}[h_n r_n(\kappa_{n_z}\sin\gamma_n$$

$$-\kappa_{n_y}\cos\gamma_n)+\frac{v'_n w'_n}{1+e_n}[w'_n\kappa_{n_x}+r_n(\kappa_{n_y}\sin\gamma_n$$

$$+\kappa_{n_z}\cos\gamma_n)]]\}\cdot\{[2(e_n+1)^2+r_n^2]h_n v'_n u''_n$$

$$+[(e_n+1)^2 v'^2_n-h_n^2[(e_n+1)^2+r_n^2]]v''_n\}$$

$$+\frac{w'_n}{r_n^3(e_n+1)^5}[r_n\kappa_{n_x}-w'_n(\kappa_{n_y}\sin\gamma_n$$

$$+\kappa_{n_z}\cos\gamma_n)]\{[2(e_n+1)^2+r_n^2]h_n v'_n u''_n$$

$$+[(e_n+1)^2 v'^2_n-h_n^2[(e_n+1)^2+r_n^2]]v''_n\}$$

$$+\frac{1}{r_n^4(e_n+1)^6}\{[(2r_n^2+w'^2_n)h_n v'_n u''_n+(v'^4_n-h_n^4$$

$$+w'^2_n v'^2_n)v''_n](e_n+1)[(v'^2_n+w'^2_n)r_n(\kappa_{n_z}\cos\gamma_n$$

$$+\kappa_{n_y}\sin\gamma_n)-h_n^2 w'_n\kappa_{n_x}]+[(v'^4_n-2h_n^4-h_n^2 v'^2_n$$

$$+w'^2_n v'^2_n)w'_n u''_n-(3r_n^2+w'^2_n)h_n w'_n v'_n v''_n$$

$$+(r_n^2-w'^2_n)h_n r_n^2 w''_n]\cdot[-h_n\kappa_{n_x}(e_n+1)v'_n$$

$$+(v'^2_n+w'^2_n)r_n(\kappa_{n_y}\cos\gamma_n-\kappa_{n_z}\sin\gamma_n)]\}\}. \quad \text{(B8)}$$

The transverse shear forces along the 2nd and 3rd axes of the cross-sectional frame of the $n$th link are, respectively, given by Equasiton's B9 and B10:

$$-B^n_{5n+5}=+\rho_n[[\dot{\Omega}^{S_n}]^T[J_{S_n}]-[\Omega^{S_n}]^T[J_{S_n}]\widetilde{\Omega}^{S_n}$$

$$-2[\omega^{B_n}]^T\underset{B_nS_n}{R}[J_{S_n}]\widetilde{\Omega}^{S_n}+2J_{S_{n_p}}[\omega^{B_n}]^T\underset{B_nS_n}{R}\widetilde{\Omega}^{S_n}$$

$$-[\omega^{B_n}]^T \underset{B_nS_n}{R}[J_{S_n}]\underset{S_nB_n}{R}\widetilde{\omega}^{B_n}\underset{B_nS_n}{R}$$

$$+[\dot{\omega}^{B_n}]^T \underset{B_nS_n}{R}[J_{S_n}]]C_n\begin{bmatrix}0 & 1 & 0\end{bmatrix}^T$$

$$-\langle\frac{(1-\nu)EJ}{(1+\nu)(1-2\nu)}\{\frac{w'_n h_n}{r_n^4(e_n+1)}\{v'^2_n\kappa_{n_x}$$

$$+\frac{h_n}{1+e_n}[v'_n r_n(\kappa_{n_y}\cos\gamma_n-\kappa_{n_z}\sin\gamma_n)$$

$$+\frac{h_n w'_n}{1+e_n}[w'_n\kappa_{n_x}+r_n(\kappa_{n_y}\sin\gamma_n+\kappa_{n_z}\cos\gamma_n)]]\}$$

$$+\frac{h_n}{r_n(e_n+1)^3}[r_n w'_n\kappa_{n_x}+\frac{h_n}{1+e_n}v'_n w'_n(\kappa_{n_y}\cos\gamma_n$$

$$-\kappa_{n_z}\sin\gamma_n)+h_n^2(\kappa_{n_z}\cos\gamma_n+\kappa_{n_y}\sin\gamma_n)]\}$$

$$+GJ\{\frac{w'_n h_n}{r_n^4(e_n+1)}\{h_n^2\kappa_{n_x}+\frac{v'_n}{1+e_n}[h_n r_n(\kappa_{n_z}\sin\gamma_n$$

$$-\kappa_{n_y}\cos\gamma_n)+\frac{v'_n w'_n}{1+e_n}[w'_n\kappa_{n_x}+r_n(\kappa_{n_y}\sin\gamma_n$$

$$+\kappa_{n_z}\cos\gamma_n)]]\}+\frac{w'_n h_n}{r_n(1+e_n)^3}[r_n\kappa_{n_x}$$

$$-w'_n(\kappa_{n_y}\sin\gamma_n+\kappa_{n_z}\cos\gamma_n)]$$

$$+\frac{v'_n}{r_n^2(e_n+1)^3}[-h_n v'_n w'_n\kappa_{n_x}$$

$$+\frac{v'_n}{1+e_n}\{v'_n w'_n r_n(\kappa_{n_y}\cos\gamma_n-\kappa_{n_z}\sin\gamma_n)$$

$$+(e_n+1)h_n[r_n(\kappa_{n_z}\cos\gamma_n+\kappa_{n_y}\sin\gamma_n)+w'_n\kappa_{n_x}]\}]$$

$$+\frac{w'_n}{r_n(e_n+1)^4}\{v'_n w'^2_n(\kappa_{n_y}\cos\gamma_n-\kappa_{n_z}\sin\gamma_n)$$

$$+(e_n+1)h_n[w'_n(\kappa_{n_y}\sin\gamma_n+\kappa_{n_z}\cos\gamma_n)$$

$$-r_n\kappa_{n_x}]\}\}\rangle'+GA_n v'_n$$

$$+\frac{(1-\nu)EJ}{(1+\nu)(1-2\nu)}\{\frac{\kappa_{n_x}}{r_n^2}[v'_n\kappa_{n_x}+\frac{h_n r_n}{1+e_n}(\kappa_{n_y}\cos\gamma_n$$

$$-\kappa_{n_z}\sin\gamma_n)]+\frac{v'_n\kappa_{n_x}}{r_n^4}\{-v'^2_n\kappa_{n_x}$$

$$+\frac{h_n}{1+e_n}[v'_n r_n(\kappa_{n_z}\sin\gamma_n-\kappa_{n_y}\cos\gamma_n)$$

$$-\frac{h_n w'_n}{1+e_n}[w'_n\kappa_{n_x}+r_n(\kappa_{n_z}\cos\gamma_n+\kappa_{n_y}\sin\gamma_n)]]\}$$

$$+\frac{h_n v'_n}{r_n^2(1+e_n)^3}[v'_n r_n\kappa_{n_x}(\kappa_{n_z}\sin\gamma_n-\kappa_{n_y}\cos\gamma_n)$$

$$-\frac{h_n}{1+e_n}[w'^2_n\kappa_{n_x}^2+r_n^2(\kappa_{n_z}^2+\kappa_{n_y}^2)$$

$$+2w'_n r_n\kappa_{n_x}(\kappa_{n_y}\sin\gamma_n+\kappa_{n_z}\cos\gamma_n)]]$$

$$+\frac{-w'_n}{r_n^6(e_n+1)^3}\{v'^2_n\kappa_{n_x}+\frac{h_n}{1+e_n}[v'_n r_n(\kappa_{n_y}\cos\gamma_n$$

$$-\kappa_{n_z}\sin\gamma_n)+\frac{h_n w'_n}{1+e_n}[w'_n\kappa_{n_x}+r_n(\kappa_{n_y}\sin\gamma_n$$

$$+\kappa_{n_z}\cos\gamma_n)]]\}\cdot\{[2(e_n+1)^2+r_n^2]h_n v'_n v''_n$$

$$+[(e_n+1)^2h_n^2-v'^2_n[(e_n+1)^2+r_n^2]]u''_n\}$$

$$+\frac{h_n}{r_n^4(e_n+1)^5}\{[-(2r_n^2+w'^2_n)h_n v'_n v''_n+(v'^4_n-h_n^4$$

$$-w'^2_n h_n^2)u''_n]h_n(w'_n\kappa_{n_x}+r_n\kappa_{n_z}\cos\gamma_n+r_n\kappa_{n_y}\sin\gamma_n)$$

$$+[(h_n^4-2v'^4_n-h_n^2v'^2_n+w'^2_n h_n^2)w'_n v''_n$$

$$-(3r_n^2+w'^2_n)h_n w'_n v'_n u''_n+(r_n^2-w'^2_n)v'_n r_n^2 w''_n]$$

$$\cdot[v'_n\kappa_{n_x}+\frac{h_n r_n}{1+e_n}(\kappa_{n_y}\cos\gamma_n-\kappa_{n_z}\sin\gamma_n)]\}\}$$

$$+GJ\{\frac{1}{r_n^2(1+e_n)}[h_n\kappa_{n_x}r_n(\kappa_{n_z}\sin\gamma_n-\kappa_{n_y}\cos\gamma_n)$$

$$+\frac{v'_n}{1+e_n}[r_n^2(\kappa_{n_y}^2+\kappa_{n_z}^2)+w'^2_n\kappa_{n_x}^2$$

$$+2w'_n\kappa_{n_x}r_n(\kappa_{n_y}\sin\gamma_n+\kappa_{n_z}\cos\gamma_n)]]$$

$$+\frac{v'_n\kappa_{n_x}}{r_n^4}\{-h_n^2\kappa_{n_x}-\frac{v'_n}{1+e_n}[h_n r_n(\kappa_{n_z}\sin\gamma_n$$

$$-\kappa_{n_y}\cos\gamma_n)+\frac{v'_n w'_n}{1+e_n}[w'_n\kappa_{n_x}+r_n(\kappa_{n_y}\sin\gamma_n$$

$$+\kappa_{n_z}\cos\gamma_n)]]\}+\frac{v'_n\kappa_{n_x}}{r_n(1+e_n)^2}[r_n\kappa_{n_x}-w'_n(\kappa_{n_y}\sin\gamma_n$$

$$+\kappa_{n_z}\cos\gamma_n)]+\frac{v'^2_n}{r_n^2(1+e_n)^3}[h_n r_n\kappa_{n_x}(\kappa_{n_y}\cos\gamma_n$$

$$-\kappa_{n_z}\sin\gamma_n)-\frac{v'_n}{1+e_n}[w'^2_n\kappa_{n_x}^2+r_n^2(\kappa_{n_y}^2+\kappa_{n_z}^2)$$

$$+2w'_n r_n\kappa_{n_x}(\kappa_{n_y}\sin\gamma_n+\kappa_{n_z}\cos\gamma_n)]]$$

$$-\frac{v'_n}{(1+e_n)^4}[r_n^2\kappa_{n_x}^2+w'^2_n(\kappa_{n_y}^2+\kappa_{n_z}^2)$$

$$
\begin{aligned}
&- 2w'_n r_n \kappa_{n_x}(\kappa_{n_y}\sin\gamma_n + \kappa_{n_z}\cos\gamma_n)]\\
&+ \frac{-w'_n}{r_n^6(e_n+1)^3}\{h_n^2\kappa_{n_x} + \frac{v'_n}{1+e_n}[h_n r_n(\kappa_{n_z}\sin\gamma_n\\
&- \kappa_{n_y}\cos\gamma_n) + \frac{v'_n w'_n}{1+e_n}[w'_n\kappa_{n_x} + r_n(\kappa_{n_y}\sin\gamma_n\\
&+ \kappa_{n_z}\cos\gamma_n)]]\}\cdot\{[2(e_n+1)^2 + r_n^2]h_n v'_n v''_n\\
&+ [(e_n+1)^2 h_n^2 - v'^2_n[(e_n+1)^2 + r_n^2]]u''_n\}\\
&+ \frac{-w'_n}{r_n^3(e_n+1)^5}[r_n\kappa_{n_x} - w'_n(\kappa_{n_y}\sin\gamma_n\\
&+ \kappa_{n_z}\cos\gamma_n)]\{[2(e_n+1)^2 + r_n^2]h_n v'_n v''_n\\
&+ [(e_n+1)^2 h_n^2 - v'^2_n[(e_n+1)^2 + r_n^2]]u''_n\}\\
&+ \frac{1}{r_n^4(e_n+1)^6}\{[(h_n^4 - 2v'^4_n - h_n^2 v'^2_n + w'^2_n h_n^2)w'_n v''_n\\
&- (3r_n^2 + w'^2_n)h_n w'_n v'_n u''_n + (r_n^2 - w'^2_n)v'_n r_n^2 w''_n]\\
&\cdot[(v'^2_n + w'^2_n)r_n(\kappa_{n_y}\cos\gamma_n - \kappa_{n_z}\sin\gamma_n)\\
&- v'_n(e_n+1)h_n\kappa_{n_x}] + [-(2r_n^2 + w'^2_n)h_n v'_n v''_n + (v'^4_n\\
&- h_n^4 - w'^2_n h_n^2)u''_n](e_n+1)[(v'^2_n + w'^2_n)r_n(\kappa_{n_y}\sin\gamma_n\\
&+ \kappa_{n_z}\cos\gamma_n) - h_n^2 w'_n\kappa_{n_x}]\}\},
\end{aligned}
\tag{B9}
$$

$$
\begin{aligned}
-B^n_{5n+6} = {}&+\rho_n[[\dot\Omega^{S_n}]^T[J_{S_n}] - [\Omega^{S_n}]^T[J_{S_n}]\widetilde\Omega^{S_n}\\
&- 2[\omega^{B_n}]^T \underset{B_nS_n}{R}[J_{S_n}]\widetilde\Omega^{S_n} + 2J_{S_{n_p}}[\omega^{B_n}]^T \underset{B_nS_n}{R}\widetilde\Omega^{S_n}\\
&- [\omega^{B_n}]^T \underset{B_nS_n}{R}[J_{S_n}]\underset{S_nB_n}{R}\widetilde\omega^{B_n}\underset{B_nS_n}{R}\\
&+ [\dot\omega^{B_n}]^T\underset{B_nS_n}{R}[J_{S_n}]]C_n\begin{bmatrix}0 & 0 & 1\end{bmatrix}^T\\
&- \langle\frac{(1-\nu)EJ}{(1+\nu)(1-2\nu)}\frac{h_n}{(e_n+1)^3}[-v'_n\kappa_{n_x}\\
&+ \frac{h_n r_n}{1+e_n}(\kappa_{n_z}\sin\gamma_n - \kappa_{n_y}\cos\gamma_n)]\\
&+ GJ\frac{1}{(e_n+1)^4}\{(e_n+1)h_n v'_n\kappa_{n_x} + r_n(\kappa_{n_z}\sin\gamma_n\\
&- \kappa_{n_y}\cos\gamma_n)(v'^2_n + w'^2_n)\}\rangle' + \langle GA_n w'_n\\
&+ \frac{(1-\nu)EJ}{(1+\nu)(1-2\nu)}\{\frac{h_n^2\kappa_{n_x}}{r_n^2(1+e_n)^2}[w'_n\kappa_{n_x}\\
&+ r_n(\kappa_{n_y}\sin\gamma_n + \kappa_{n_z}\cos\gamma_n)]\\
&+ \frac{w'_n h_n}{r_n^2(1+e_n)^3}[v'_n r_n\kappa_{n_x}(\kappa_{n_z}\sin\gamma_n - \kappa_{n_y}\cos\gamma_n)\\
&- \frac{h_n}{1+e_n}[w'^2_n\kappa^2_{n_x} + r_n^2(\kappa^2_{n_z} + \kappa^2_{n_y})\\
&+ 2w'_n r_n\kappa_{n_x}(\kappa_{n_y}\sin\gamma_n + \kappa_{n_z}\cos\gamma_n)]]\\
&+ \frac{1}{r_n^2(e_n+1)^3}(h_n v''_n - v'_n u''_n)\{v'^2_n\kappa_{n_x}\\
&+ \frac{h_n}{1+e_n}[v'_n r_n(\kappa_{n_y}\cos\gamma_n - \kappa_{n_z}\sin\gamma_n)\\
&+ \frac{h_n w'_n}{1+e_n}[w'_n\kappa_{n_x} + r_n(\kappa_{n_y}\sin\gamma_n + \kappa_{n_z}\cos\gamma_n)]]\}\\
&+ \frac{h_n}{r_n^2(e_n+1)^5}\{[(r_n^2 - w'^2_n)(h_n u''_n + v'_n v''_n)\\
&+ 2r_n^2 w'_n w''_n][v'_n\kappa_{n_x} + \frac{h_n r_n}{1+e_n}(\kappa_{n_y}\cos\gamma_n - \kappa_{n_z}\sin\gamma_n)]\\
&+ (v'_n u''_n - h_n v''_n)(e_n+1)w'_n\frac{h_n}{1+e_n}[w'_n\kappa_{n_x}\\
&+ r_n(\kappa_{n_z}\cos\gamma_n + \kappa_{n_y}\sin\gamma_n)]\}\}\\
&+ GJ\{\frac{1}{(1+e_n)^2}[w'_n[\frac{v'^2_n}{r_n^2}\kappa^2_{n_x} + (\kappa^2_{n_y} + \kappa^2_{n_z})]\\
&- \frac{h_n^2\kappa_{n_x}}{r_n}(\kappa_{n_y}\sin\gamma_n + \kappa_{n_z}\cos\gamma_n)]\\
&+ \frac{v'_n w'_n}{r_n^2(1+e_n)^3}[h_n r_n\kappa_{n_x}(\kappa_{n_y}\cos\gamma_n - \kappa_{n_z}\sin\gamma_n)\\
&- \frac{v'_n}{1+e_n}[w'^2_n\kappa^2_{n_x} + r_n^2(\kappa^2_{n_y} + \kappa^2_{n_z})\\
&+ 2w'_n r_n\kappa_{n_x}(\kappa_{n_y}\sin\gamma_n + \kappa_{n_z}\cos\gamma_n)]]\\
&- \frac{w'_n}{(1+e_n)^4}[r_n^2\kappa^2_{n_x} + w'^2_n(\kappa^2_{n_y} + \kappa^2_{n_z})\\
&- 2w'_n r_n\kappa_{n_x}(\kappa_{n_y}\sin\gamma_n + \kappa_{n_z}\cos\gamma_n)]\\
&+ \frac{1}{r_n^2(e_n+1)^3}(h_n v''_n - v'_n u''_n)\{h_n^2\kappa_{n_x}\\
&+ \frac{v'_n}{1+e_n}[h_n r_n(\kappa_{n_z}\sin\gamma_n - \kappa_{n_y}\cos\gamma_n)\\
&+ \frac{v'_n w'_n}{1+e_n}[w'_n\kappa_{n_x} + r_n(\kappa_{n_y}\sin\gamma_n + \kappa_{n_z}\cos\gamma_n)]]\}
\end{aligned}
$$

$$+\frac{r_n}{(1+e_n)^5}(h_n v_n'' - v_n' u_n'')[r_n\kappa_{n_x} - w_n'(\kappa_{n_y}\sin\gamma_n$$

$$+\kappa_{n_z}\cos\gamma_n)] + \frac{1}{r_n^2(e_n+1)^6}\{(v_n' u_n''$$

$$- h_n v_n'')(e_n+1)w_n'[r_n(v_n'^2 + w_n'^2)(\kappa_{n_y}\sin\gamma_n$$

$$+\kappa_{n_z}\cos\gamma_n) - h_n^2 w_n'\kappa_{n_x}] + [(r_n^2 - w_n'^2)(h_n u_n''$$

$$+ v_n' v_n'') + 2r_n^2 w_n' w_n''][r_n(v_n'^2 + w_n'^2)(\kappa_{n_y}\cos\gamma_n$$

$$-\kappa_{n_z}\sin\gamma_n) - h_n v_n'\kappa_{n_x}(e_n+1)]\}\}\rangle. \tag{B10}$$

The agent variables $\bar{B}^n_{5n+4}$ is given by Equation B11:

$$-\bar{B}^n_{5n+4} = \frac{(1-\nu)EJ}{(1+\nu)(1-2\nu)}\{-\frac{w_n' v_n'}{r_n^4(e_n+1)}\{v_n'^2\kappa_{n_x}$$

$$+\frac{h_n}{1+e_n}[v_n' r_n(\kappa_{n_y}\cos\gamma_n - \kappa_{n_z}\sin\gamma_n)$$

$$+\frac{h_n w_n'}{1+e_n}[w_n'\kappa_{n_x} + r_n(\kappa_{n_y}\sin\gamma_n + \kappa_{n_z}\cos\gamma_n)]]\}$$

$$+\frac{h_n^2}{r_n^2(e_n+1)^3}\{v_n' w_n'\kappa_{n_x}$$

$$+\frac{1}{1+e_n}\{h_n w_n' r_n(\kappa_{n_y}\cos\gamma_n - \kappa_{n_z}\sin\gamma_n)$$

$$-(e_n+1)v_n'[r_n(\kappa_{n_y}\sin\gamma_n + \kappa_{n_z}\cos\gamma_n)$$

$$+ w_n'\kappa_{n_x}]\}\}\} + GJ\{-\frac{w_n' v_n'}{r_n^4(e_n+1)}\{h_n^2\kappa_{n_x}$$

$$+\frac{v_n'}{1+e_n}[h_n r_n(\kappa_{n_z}\sin\gamma_n - \kappa_{n_y}\cos\gamma_n)$$

$$+\frac{v_n' w_n'}{1+e_n}[w_n'\kappa_{n_x} + r_n(\kappa_{n_y}\sin\gamma_n + \kappa_{n_z}\cos\gamma_n)]]\}$$

$$+\frac{1}{r_n(e_n+1)^4}(v_n'^2 + w_n'^2)[h_n w_n'(\kappa_{n_y}\cos\gamma_n$$

$$-\kappa_{n_z}\sin\gamma_n) - (e_n+1)v_n'(\kappa_{n_y}\sin\gamma_n + \kappa_{n_z}\cos\gamma_n)]$$

$$-\frac{w_n' v_n'}{r_n(1+e_n)^3}[r_n\kappa_{n_x} - w_n'(\kappa_{n_y}\sin\gamma_n + \kappa_{n_z}\cos\gamma_n)]\}. \tag{B11}$$

The bending moments about the 3rd and the 2nd axes of the cross-sectional frame of the $n$th link are, respectively, given by Equation's B12 and B13:

$$-\bar{B}^n_{5n+5} = \frac{(1-\nu)EJ}{(1+\nu)(1-2\nu)}\{\frac{w_n' h_n}{r_n^4(e_n+1)}\{v_n'^2\kappa_{n_x}$$

$$+\frac{h_n}{1+e_n}[v_n' r_n(\kappa_{n_y}\cos\gamma_n - \kappa_{n_z}\sin\gamma_n)$$

$$+\frac{h_n w_n'}{1+e_n}[w_n'\kappa_{n_x} + r_n(\kappa_{n_y}\sin\gamma_n + \kappa_{n_z}\cos\gamma_n)]]\}$$

$$+\frac{h_n}{r_n^2(e_n+1)^3}[\kappa_{n_x} v_n'^2 w_n'$$

$$+\frac{h_n}{1+e_n}[+v_n' w_n' r_n(\kappa_{n_y}\cos\gamma_n - \kappa_{n_z}\sin\gamma_n)$$

$$+(e_n+1)h_n(w_n'\kappa_{n_x} + r_n\kappa_{n_z}\cos\gamma_n$$

$$+ r_n\kappa_{n_y}\sin\gamma_n)]]\} + GJ\{\frac{w_n' h_n}{r_n^4(e_n+1)}\{h_n^2\kappa_{n_x}$$

$$+\frac{v_n'}{1+e_n}[h_n r_n(\kappa_{n_z}\sin\gamma_n - \kappa_{n_y}\cos\gamma_n)$$

$$+\frac{v_n' w_n'}{1+e_n}[w_n'\kappa_{n_x} + r_n(\kappa_{n_y}\sin\gamma_n + \kappa_{n_z}\cos\gamma_n)]]\}$$

$$+\frac{1}{r_n(e_n+1)^4}\{v_n' w_n'(v_n'^2 + w_n'^2)(\kappa_{n_y}\cos\gamma_n$$

$$-\kappa_{n_z}\sin\gamma_n) + (e_n+1)h_n[(v_n'^2 + w_n'^2)(\kappa_{n_y}\sin\gamma_n$$

$$+\kappa_{n_z}\cos\gamma_n) - r_n w_n'\kappa_{n_x}]\} + \frac{w_n' h_n}{r_n(1+e_n)^3}[r_n\kappa_{n_x}$$

$$- w_n'(\kappa_{n_y}\sin\gamma_n + \kappa_{n_z}\cos\gamma_n)]\}, \tag{B12}$$

$$-\bar{B}^n_{5n+6} = \frac{(1-\nu)EJ}{(1+\nu)(1-2\nu)}\{\frac{h_n}{(e_n+1)^3}[-v_n'\kappa_{n_x}$$

$$+\frac{h_n r_n}{1+e_n}(\kappa_{n_z}\sin\gamma_n - \kappa_{n_y}\cos\gamma_n)]\}$$

$$+ GJ\frac{1}{(e_n+1)^3}[h_n v_n'\kappa_{n_x}$$

$$+\frac{r_n(v_n'^2 + w_n'^2)}{e_n+1}(\kappa_{n_z}\sin\gamma_n - \kappa_{n_y}\cos\gamma_n)]. \tag{B13}$$